On the Machining of Involute Helical Gears - Prediction models on tool geometry, cut gear tooth surface topography, chip geometry, and tool cutting forces

Svahn, Mattias

LUND UNIVERSITY

PO Box 117
221 00 Lund
+46 46-222 00 00

On the Machining of Involute Helical Gears

Prediction models on tool geometry, cut gear tooth surface topography, chip geometry, and tool cutting forces

MATTIAS SVAHN

LUND UNIVERSITY

DOCTORAL THESIS

Division of Machine Elements
Department of Mechanical Engineering
Lund University
Lund, Sweden 2016

ISBN 978-91-7623-610-9 (print)
ISBN 978-91-7623-611-6 (pdf)
LUTMDN/TMME–1020–SE (2016)
Printed in Sweden by Media-Tryck, Lund University
Lund 2016

Preface

The research leading to this thesis has been carried out at the division of Machine Elements at Lund University from December 2010 to January 2016. The first part, December 2010 to 2013, has been financed by ProViking/SSF, together with the partner companies Volvo Construction Equipment, Volvo Power Train, Sandvik Coromant, and Swepart Transmission AB. The support is gratefully acknowledged.

First and foremost I like to thank my supervisor professor Carin Andersson for being a great supervisor these years. I like to thank my co-supervisor associate professor Lars Vedmar. I have enormously benefited from Lars broad knowledge in involute gearing, machine elements, and engineering in general. Several inspiring and fruitful discussions with my supervisors are the foundation of this work.

I wish to express my gratitude to the employees at our partner companies

Volvo Construction Equipment:	Magnus E. Andersson, Joakim Holm, Hugo Limachi
Volvo Power Train:	Per Elandersson, Mattias Åkerlund
Sandvik Coromant:	Willy Åström, Mats Wennmo, Sören Sjöberg, Kenneth Sundberg
Swepart Transmission AB:	Hans Hansson

Without your support, my thesis would lack the industrial connection, relevance, and applicability.

Abstract

The modern requirements on power transmissions focus on energy efficiency, low noise and dynamic vibrations, and power density. In order to meet these requirements, the gear wheels must be manufactured to very high precision. Additionally, it should be economical to manufacture these gears within the tight requested tolerances. Gears manufactured within automotive, truck, and construction equipment are usually cut using milling tools. The profile accuracy and the surface roughness achieved after manufacturing, which determines the gear quality, are connected to the process parameters and possible manufacturing related errors. Prediction models to accurately determine gear quality, where tool and process related errors are taken into account, are needed in order to improve the manufacturing process. Tool life has also a strong economic impact in machining operations. Tool life prediction is an important part in optimization of the machining processes, where tool life is strongly connected the cutting forces and the geometry of the cut chips.

In this work mathematical models are established in parametric form, based on analytical differential description. These models are developed in order to increase knowledge and understanding of the complex machining processes involved in gear manufacturing. Focus is on the cut gear tooth surface quality, and on milling related topics, such as cut chip geometry, tool cutting forces, and tool wear prediction.

The mathematical models are used in a number of experimental studies presented in this thesis. The experimental studies were performed in industrial conditions, where tool and process related errors that are common in industrial applications have been considered. The correlation is very good, which shows the industrial applicability of the presented models.

Keywords: Gear hobbing; Gear milling; Chip geometry; Cutting forces; Surface topography; Tool wear.

Appended publications

Paper I

Mattias Svahn, Lars Vedmar, and Carin Andersson,
Tooth Deviation of an Involute Helical Gear Manufactured in a Simulated Hobbing Process with Introduced Errors,
CIRP 1st International Conference on Virtual Machining Process Technology, 2012, Montreal, Canada.

Paper II

Mattias Svahn, Lars Vedmar, and Carin Andersson,
The Influence of Tool Tolerances on the Gear Quality of a Gear Manufactured by an Indexable Insert Hob,
VDI International Conference on Gears, 2013, Garching, Münich, Germany.
(Republished by invitation in Gear Technology, July, 2014, Vol. 31, No. 5)

Paper III

Mattias Svahn, and Lars Vedmar,
Prediction of Alignment Deviations on a Lead Crowned Helical Gear Manufactured by a Hob,
International Journal of Manufacturing Research, 2014, Vol. 9, No. 1, pp. 58–73.

Paper IV

Mattias Svahn, Lars Vedmar, and Carin Andersson,
Gear Tooth Surface Roughness of Helical Gears Manufactured by a Form Milling Cutter,
International Gear Conference, 2014, Lyon, France.
(Republished by invitation in Gear Technology, September/October, 2015, Vol. 32, No. 7)

Paper V

Mattias Svahn,
The Undercut Criterion of Pinion Shaper Cutters — and an Improvement by Modifying the Basic Rack Profile,
ASME Journal of Manufacturing Science and Engineering 2015, Vol. 138, No. 1, pp. 011011-1 — 011011-8.

Paper VI

Mattias Svahn, Carin Andersson, and Lars Vedmar,
Prediction and Experimental Verification of the Cutting Forces in Gear Form Milling,
Springer, The International Journal of Advanced Manufacturing Technology, 2015

Paper VII

Mattias Svahn, Lars Vedmar and Carin Andersson,
Prediction of the cutting forces in gear hobbing and the wear behavior of the individual hob cutting teeth,
Under 2nd review: Springer, The International Journal of Advanced Manufacturing Technology

Author's contributions to appended publications

Paper I

Svahn took part in planning, developed the mathematical model, performed simulations and analysis. Major part in writing publication. Experiments and measurements were assisted by the partner company.

Paper II

Svahn took major part in planning, developed the mathematical model, performed simulations and analysis. Major part in writing publication. Experiments and measurements were assisted by the partner company.

Paper III

Co-author performed analytical analysis. Svahn performed simulations, analysis, and major part in writing publication. Measurements were assisted by the partner company.

Paper IV

Svahn took major part in planning, developed the mathematical model, performed simulations and analysis. Major part in writing publication. Experiments and measurements were assisted by the partner company.

Paper V

Single author.

Paper VI

Svahn took major part in planning, developed the mathematical model, performed simulations and analysis. Major part in writing publication. Experiments and measurements were assisted by the partner company.

Paper VII

Svahn took major part in planning, developed the mathematical model, performed simulations and analysis. Major part in writing publication.

Contents

List of Symbols

a	Center distance
$b = b_0\, m_\mathrm{n}$	Gear face width
c_a	Measured tip relief
c_β	Measured lead crowning
C	Designed lead crowning
$f_{\mathrm{f},\alpha}, f_{\mathrm{f},\beta}$	Measured form deviation, involute and lead resp.
$f_{\mathrm{g},\alpha}, f_{\mathrm{H},\beta}$	Measured alignment deviation, involute and lead resp.
F_α, F_β	Measured total deviation, involute and lead resp.
$F_\mathrm{c},\ F_\mathrm{t}$	Cutting force, cutting and thrust direction resp.
g	Number of hob entrances
$h = h_0\, m_\mathrm{n}$	Chip thickness, Distance from ideal smooth surface to cut surface
$h_\mathrm{a} = h_{0,\mathrm{a}}\, m_\mathrm{n}$	Addendum height (basic rack)
$h_\mathrm{e} = h_{0,\mathrm{e}}\, m_\mathrm{n}$	Mean chip thickness
h_max	Maximum chip thickness
$h_\mathrm{p} = h_{0,\mathrm{p}}\, m_\mathrm{n}$	Protuberance height (basic rack)
$h_\mathrm{t} = h_{0,\mathrm{t}}\, m_\mathrm{n}$	Dedendum height (basic rack)
$h_\mathrm{tc} = h_{0,\mathrm{tc}}\, m_\mathrm{n}$	Tip chamfer height (basic rack)
i, j	Identification number of cutting edge
K	Wear constant (Archard's wear model)
$K_{\mathrm{c,c}}, K_{\mathrm{t,c}}$	Cutting force coefficient, cutting and thrust direction resp.
$K_{\mathrm{c,e}}, K_{\mathrm{t,e}}$	Edge force coefficient, cutting and thrust direction resp.
m_n	Normal module
n	Number of cutting teeth per hob revolution, Total number of cutting teeth (form milling cutter)
n, n_1, n_2, n_3	Constants (Taylor tool life equation)
N	Total number of cutting teeth (hob), Normal force (Archard's wear model)
p	Contact pressure (Archard's wear model)

r_{b}	Radius of base circle
$r_{\mathrm{t}} = r_{0,\mathrm{t}}\, m_{\mathrm{n}}$	Fillet radius (basic rack)
$R_{\mathrm{bot}} = R_{0,\mathrm{bot}}\, m_{\mathrm{n}}$	Bottom radius
$R_{\mathrm{t}} = R_{0,\mathrm{t}}\, m_{\mathrm{n}}$	Reference radius $R_{\mathrm{t}} = m_{\mathrm{n}} z/2/\cos\beta$
$R_{\mathrm{tip}} = R_{0,\mathrm{tip}}\, m_{\mathrm{n}}$	Outer radius
s	Feed per tooth (form milling cutter), Rolled distance, Chip length (Sliding distance in Archard's wear model)
S	Feed per gear revolution (hob), Feed per tool revolution (form milling cutter)
$S_{\mathrm{i}}, S_{\mathrm{j}}$	Surface cut by cutting edge i, j resp.
T	Time (Taylor tool life equation)
v_{c}	Cutting speed
V	Worn volume (Archard's wear model)
VB	Tool flank wear *(German: "verschleißmarkenbreite")*
w	Chip width
xm_{n}	Addendum modification
z	Gear tooth number
α_{n}	Normal pressure angle (basic rack)
α_{tc}	Tip chamfer angle (basic rack)
α_{p}	Protuberance angle (basic rack)
β	Helical angle (basic rack)
γ	Hook angle of cutting tooth (hob)
γ_{maj}	Major cutting edge angle
γ_{min}	Minor cutting edge angle
δ_1, δ_2	Tip relief parameters (basic rack)
$\Delta = \Delta_0\, m_{\mathrm{n}}$	Grinding stock (basic rack)
θ	Auxiliary angle for elliptical fillet (basic rack)
κ	Gash angle of cutting tooth (hob)
λ	Lead angle (hob)
ϕ	Tool rotational angle (hob, form milling cutter)
$\Delta\phi$	Angle between cutting teeth (hob, form milling cutter)
ψ	Gear rotational angle
$\mathbf{r}$	Position vector
$\mathbf{n}$	Normal vector

$\xi_{\mathrm{n}}, \eta_{\mathrm{n}}$	Basic rack coordinates (non-dimensional)
ξ, η, ζ	Cartesian coordinates (non-dimensional)
X, Y, Z	Cartesian coordinates

Subscripts

g	Gear
h	Hob
s	Shaper cutter
SCP	Start control point
ECP	End control point

Part I

Chapter 1

Introduction

The gear is an old machine element, which have been around for at least 5000 years [1]. For a very long period of time the gear material was wood, or metal rims with wooden gear teeth, as these gear types could withstand shock loads better than cast iron gears. Metal gears for power transmissions are much more recent, emerging at end of 18th century. However, metal gears were used in clocks for a long time beforehand.

This thesis is on machining of cylindrical involute helical gears. The first known machine to cut gears was invented approximately 1540 A.D. by the Italio-Spanish clockmaker Juanelo Torriano. The gear tools and manufacturing methods emphasized on in this thesis were invented much later. The form milling cutter was invented around 1783 by Samuel Rehé. The first patents on the hob were taken around 1835 by Joseph Whitworth in England. In 1895 the gear shaper cutter was developed by Fellows Corporation U.S.A (E. R. Fellows), and this method is still referred to as the Fellows' method.

The mathematical theory of gear tooth action started around 1600. Leonard Euler (1707-1783), who is considered the father of involute gearing, worked out the design principles and the rules for conjugate action. Gears with involute tooth profile is by far the most used gear type in mechanical power transmissions. Reasons are that involute gears transmit motion uniformly, the involute profile is insensitive to changes in center distance, and that involute gears can be generated accurately with inexpensive and universal tools.

In the present time, extensive research is carried out within gearing, including topics such as gear manufacturing, gear dynamics, and gear strength.

1.1 Background

Gears are used to transmit motion and power, where the main application is to either:

- Increase or decrease speed
- Increase force/torque
- Move motion from one place to an other

Other transmission alternatives meet the above mentioned criteria, but gears are preeminent by its compact design and energy efficient way to transmit motion and power.

The drivelines in automotive, truck, and construction equipment contain several gear wheels. Multiplying the amount of these gear wheels with the annual production of the vehicles gives an idea of the number of gears produced annually, within these sectors alone. Gears are predominant in several other sectors, such as energy production, industrial machines etc., where gear wheels are produced in high production volumes. Most of these gear wheels are cut using milling or cutting tools, case hardened, and refined in subsequent processes. The industrial strive is to make mechanical power transmissions that are energy efficient, generates low noise and dynamic vibration, and with high power density. To achieve these aims, the gear wheels must be manufactured to very high precision.

Additionally, it should be economical to manufacture these gears within the tight requested tolerances. To be able to improve the manufacturing steps, deep knowledge and understanding of the manufacturing processes are needed. The possibility to in advance determine the expected gear quality after manufacturing will open up for optimization, for example, to adequately choose process parameters based on this new knowledge. Tool and process related errors that are common in industrial conditions must be taken into account as they will directly affect the gear quality. Moreover, to increase productivity, which is economically beneficial, new tool concepts are recently introduced on the market that utilize the potential of carbide cutting tools. These tools are able to operate at significantly higher cutting speeds and feed rates. However, these tools are more prone to geometrical errors compared to their high speed steel equivalent. These possible errors will affect the accuracy of the cut gear and the machining performance, and must therefore be controlled.

Tool performance is also of strong economical importance. One of several tool performance indicators is tool life. A long tool life is desired as it reduce tool related costs, such as tool cost, tool handling cost, resharpening cost, etc., as well as process related costs, such as setup time due to tool changes. Tool wear limits the tool life. The tool load, such as the tool cutting forces and and the geometry of the cut chips, is the foundation of tool wear prediction models. If tool wear can be modeled and predicted, this knowledge can be used and applied in strategies in order to prolong tool life. To extend tool life and to increase tool utilization would benefit manufacturing economy.

1.2 Objectives

Figure 1.1 shows an overview of the research presented in this thesis. The thesis comprises several topics on the manufacturing of cylindrical involute gears, where the gear is manufactured in a milling operation. The aim is to develop predictive models to determine the gear quality, the tool cutting forces, and the tool wear, which all influence manufacturing economy.

The objectives of this thesis are twofold. One objective is to study the machined tooth surface given the tool design and the process parameters. By the finite number of cuts made by the tool in combination with the feed, the machined tooth surface will deviate from the ideal smooth tooth surface. Possible tool and machining errors will give additional tooth surface errors. To be able to predict the machined tooth surface in advance gives the possibility to determine the expected gear tooth quality achievable from the milling operation.

The other objective is to study how the tool is affected in the milling operation, by the chip geometry each cutting edge will remove, the cutting forces acting on the tool cutting edge when these chips are sheared off, and the wear that will progress on the tool cutting edge during machining. If these things can be modeled and be predicted they can also be controlled, which gives the possibility to optimize tool utilization.

The dimensions of interest are very small compared to the gear and the tool, especially the gear tooth surface deviation and the chip thickness. A method is needed to determine these accurately, without numerical inaccuracies. The approach to reach the objectives is to build parametric mathematical models using an analytical differential description to keep numerical errors to a minimum. By this it is possible to solve the gear tooth surface topography and the chip thickness directly without using differences between nearly equal figures.

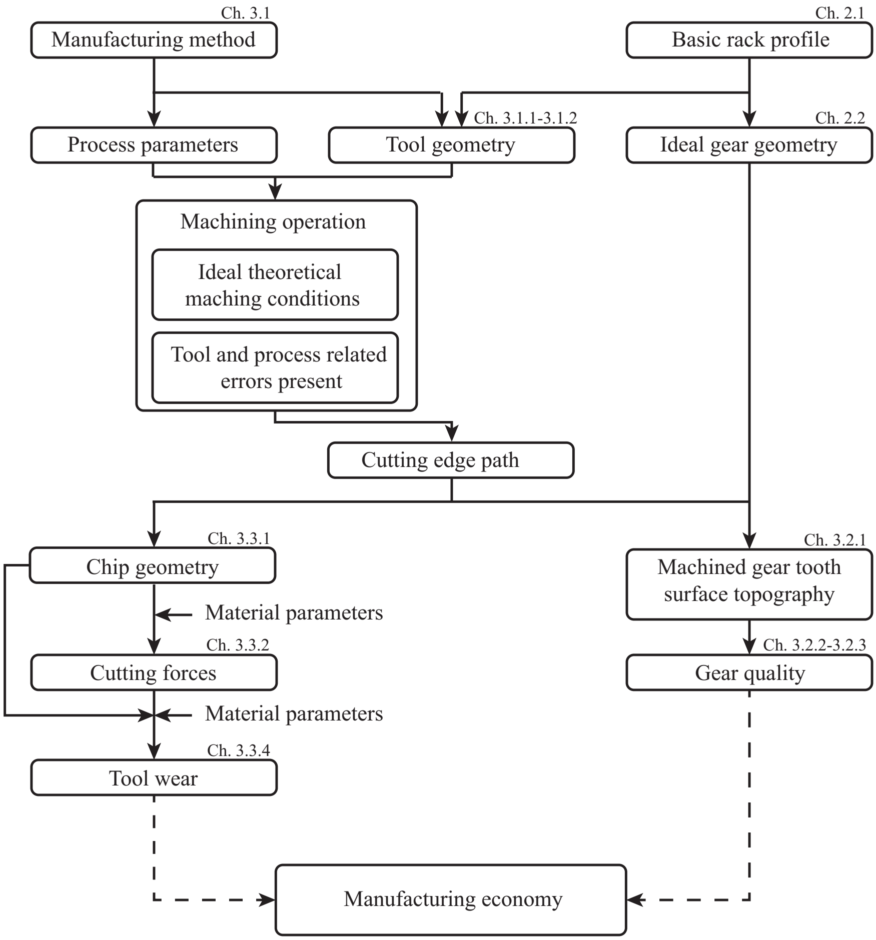

Figure 1.1: Overview of research presented in this thesis. References are made to the corresponding chapters.

The main research questions for this thesis are formulated as:

- R. Q. 1: Is it possible, by using analytical mathematical models, to predict the gear tooth topography and the gear quality of the machined gear?
- R. Q. 2: Is it possible, by using analytical mathematical models, to predict the tool cutting forces and the tool wear of each individual hob cutting tooth in the gear hobbing process?

1.3 Scope and Limitations

Neglecting deformations of the work piece and the tool, the determination of the machined gear tooth surface topography and the cut chip geometry are purely geometrical. In ideal conditions, tool type, tool geometry, gear geometry, and process parameters are needed. In industrial conditions, however, errors related to the tool and the machine are common and must be taken into account, as these possible errors will affect both the machined tooth surface and the machining performance. Several parameters that affect the gear machining process are shown in Fig. 1.2.

Milling tools experience both forced and self-excited vibrations during machining operations due to the intermittent machining conditions. If the system is excited it will result in chatter vibrations, that will affect the tooth surface topography, the chip geometry, and consequently the cutting forces. Machine dynamics, by possible vibrations, are beyond the scope of this thesis. However, if the systems are stable, as were the case in the experimental studies performed in this thesis, machine vibrations can be neglected.

The cutting forces needed for the chip removal are, besides the instantaneous chip area, connected to the material being cut, and the friction in the tool and the chip interface. These are considered in the material constants in the cutting force model. The material constants are considered as bulk parameters, no consideration is taken to variation in the raw material, such as cutting direction in relation to the gear blank (isotropic material is assumed), batch variations, etc..

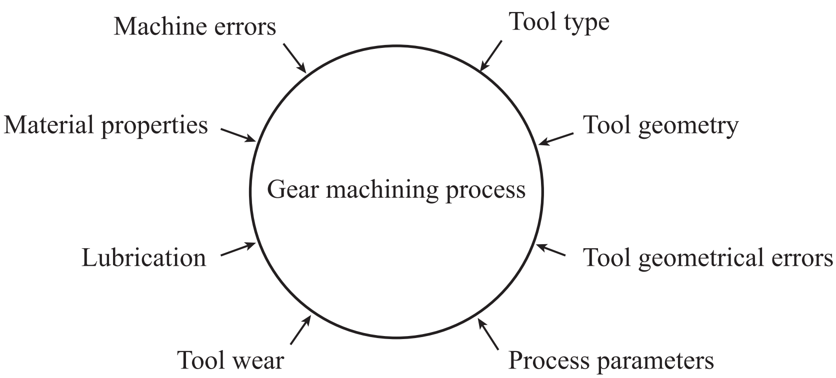

Figure 1.2: Influencing sub-systems on the gear milling process.

1.4 Research Outline

The research in this thesis can be categorized in three main subject.

The first is on the tool design. To be able to manufacture the intended gear geometry correctly, it is of uttermost importance that the tool has the proper geometry. The tool should share a mutual basic rack with the gear to produce. One problem that was discovered, however, is that the tool tip can in some cases be undercut, and an undercut tool will not produce the correct geometry. In paper V an analysis is presented on how to avoid this type of undercut. The second subject is on prediction of the machined tooth surface topography. Prediction of the tooth surface topography in hobbing is treated in paper I, II, and III, and in gear form milling in paper IV. In these papers, the machined gear tooth surface topography is predicted and experimentally verified, where various production and tool related errors are considered. These two subjects are connected to R. Q. 1.

The third main subject is on prediction of the chip geometry, the cutting forces, and the wear behavior that progress on the tool during machining operation, which is connected to R. Q. 2. Since it is difficult to measure and validate the cutting forces in gear hobbing, and especially the cutting forces on each individual hob cutting tooth, a diversion was made to initially study the less complex gear form milling operation. A model was developed where the cutting forces in gear form milling are predicted. The cutting forces in gear form milling could easier be validated in an experimental study, see paper

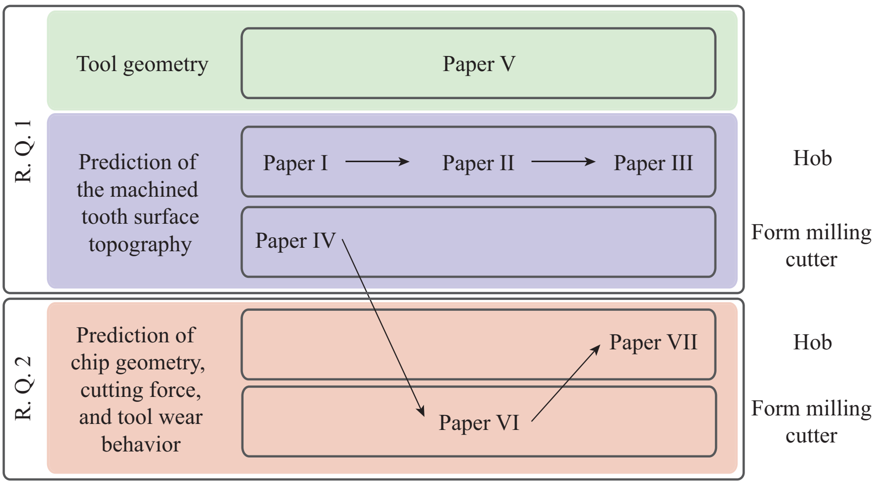

Figure 1.3: Research Outline

VI. The gained knowledge was then used to support the development of the model for predicting cutting forces and tool wear in gear hobbing, which is presented in paper VII.

The appended papers are outlined in Fig. 1.3, where the three research subjects are presented. This figure also illustrates how these papers are connected within research context, and how work progression and knowledge is transfer to the subsequent publications. A summary of each appended paper is presented in Ch. 4, where paper I, II, III, IV and V focus on R. Q. 1, and paper VI and VII focus on R. Q. 2.

Chapter 2

Geometry of Involute Cylindrical Gears

The geometry of involute helical gears can be defined in numerous ways. The method mostly used in industry is to define the geometry of the basic member instead of defining the gear geometry directly. For cylindrical involute gears, the basic member is the basic rack profile. Using the basic rack to describe the gear geometry is convenient as the basic rack description is independent of the manufacturing method. Possible modifications to the gear tooth, such as tip relief, tip chamfer, and protuberance, are easily added to the basic rack. The design methodology is unified by the basic rack, which makes it easier for the manufacturer to find the tool geometry. The requirement to cut the intended gear geometry is that the tool and the gear are conjugated to a mutual basic rack design.

2.1 Basic Rack Design

The profile of the basic rack is defined in its normal section. In this section the basic rack pitch equals πm_{n}. The median line of the basic rack is positioned where the distance between neighboring tooth flanks equals one half of the basic pitch. i.e. $\pi m_{\mathrm{n}}/2$, see Fig. 2.1. From the median line, the dedendum height $h_{\mathrm{t}} = h_{0,\mathrm{t}} m_{\mathrm{n}}$ and the addendum height $h_{\mathrm{a}} = h_{0,\mathrm{a}} m_{\mathrm{n}}$ are defined. In the normal section, the profile pressure angle is α_{n}.

Fig. 2.1 shows the basic rack in the normal plane. This rack has sharp corners in the fillet. The normal situation for heavily loaded gear teeth is that the gear must have a controlled fillet geometry in order to optimize the gear strength. To increase gear strength, the basic rack fillet is most often

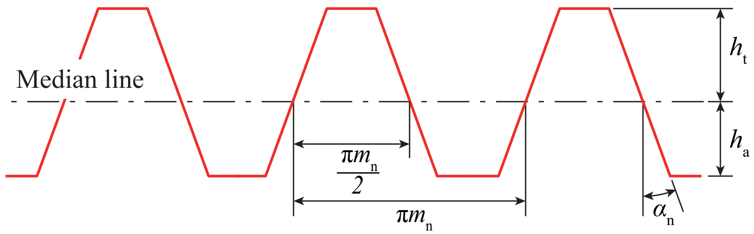

Figure 2.1: Normal section of the basic rack profile.

specified by a circular sector with the fillet radius $r_t = r_{0,t} m_n$. To specify a basic rack fillet radius is, however, not an requirement.

The standard basic rack, with a fillet radius, is shown in the left part of Fig. 2.2, see, for example, DIN 867 [2]. The design parameters are made non-dimensional by division with the normal module m_n. The basic rack parameters are standardized. However, they are often changed compared to the standard values in order to optimize the gear set, with respect to contact ratio, gear strength, etc..

Further, the basic rack profile is often modified to define tooth profiles desired for optimum gear meshing. As the gear tooth deforms in operation, one example is to add tip relief which permits interference-free tooth engaging between mating gears [3]. Another example is to add tip chamfer to, for example, protect the tooth flank from handling damages [4]. Detailed geometrical description of these types of modifications, among others, are

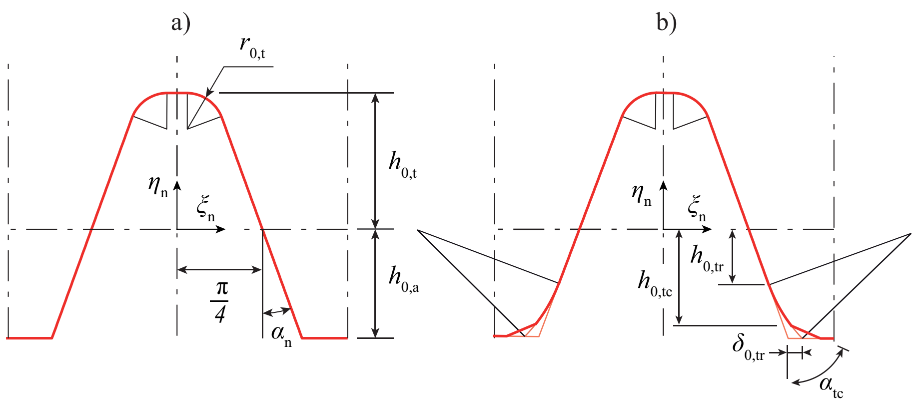

Figure 2.2: Basic rack profile. The standard basic rack design to the left, and basic rack with tip relief and tip chamfer to the right.

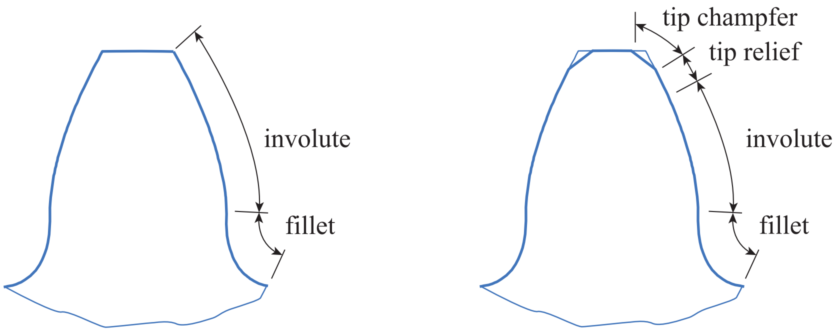

Figure 2.3: Conjugate gear tooth profiles to basic rack in Fig. 2.2.

presented in industrial standards, for example, in SMS [5, 6]. Tip relief and tip chamfer, which obviously also can be added separately, are incorporated to the basic rack shown in the right part of Fig. 2.2. Here $h_{0,\mathrm{tr}}$ and $\delta_{0,\mathrm{tr}}$ are tip relief parameters, and $h_{0,\mathrm{tc}}$ and α_{tc} are tip chamfer parameters. The conjugate gear tooth profile to the standard basic rack, and the rack with tip relief and tip chamfer are shown in Fig. 2.3 respectively.

As will be shown later, the cut gear tooth surface will deviate from the ideal smooth conjugate tooth surface. Even using a perfect tool, tooth surface errors will be present on the cut gear tooth due to the feed and the finite number of cuts. Additional errors will be present using non-perfect tools. These surface errors are not desired in high performance gearing, therefore, the gear tooth surfaces are most often refined in a subsequent

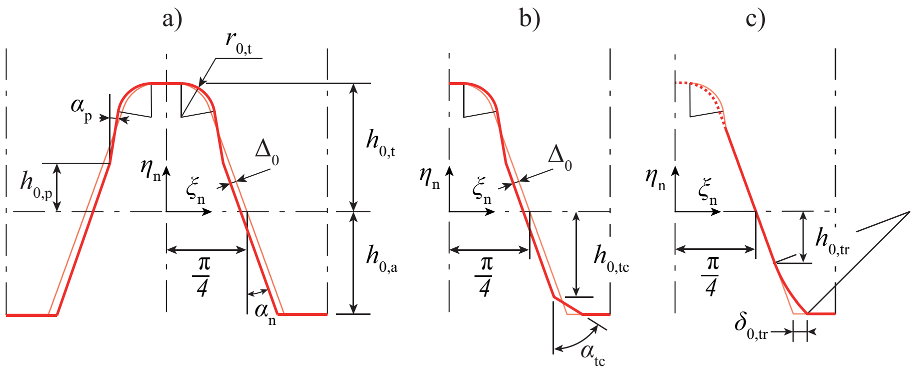

Figure 2.4: Basic rack profile with protuberance. a) the standard basic rack design (for the rough cut), b) basic rack with tip chamfer (for the rough cut), and c) basic rack with tip relief (for the finishing cut).

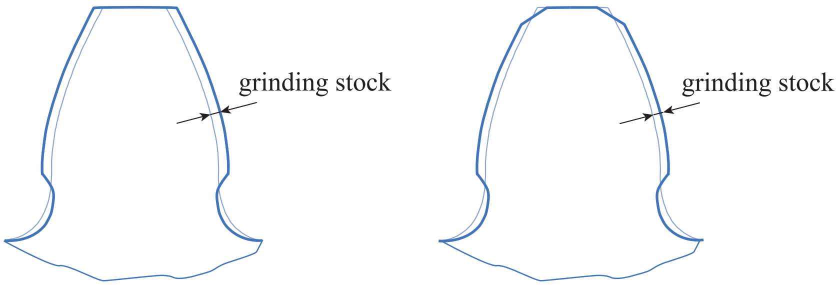

Figure 2.5: Conjugate gear tooth profiles to the basic racks ”a” and ”b” in Fig. 2.4

operation. In preparation of subsequent refining steps, the gear teeth are cut using a protuberance tool. This tool leaves a thin slice of material behind, i.e. grinding stock or machining allowance, on the gear tooth flanks. The amount of grinding stock should be sufficient to swallow the imperfections from the roughing cut. However, to support the time consuming and cost intensive refining processes, this grinding stock should preferably be kept to a minimum. The fillet is rarely refined, only the involute and the possible tip relief regions are resurfaced. To get a controlled transition between the fillet and the involute profile, the gear tooth is also intentionally undercut by this protuberance tool. In Fig. 2.4a and Fig. 2.4b protuberance is added to the basic rack profile, for the standard basic rack and the basic rack with tip chamfer, respectively. Figure 2.4c shows the basic rack of the refining tool, where tip relief is added. Figure 2.5 shows the conjugate tooth profiles to the basic racks shown in Fig. 2.4a and Fig. 2.4b. This figure shows the grinding stock left behind on the tooth flanks and the undercut fillet.

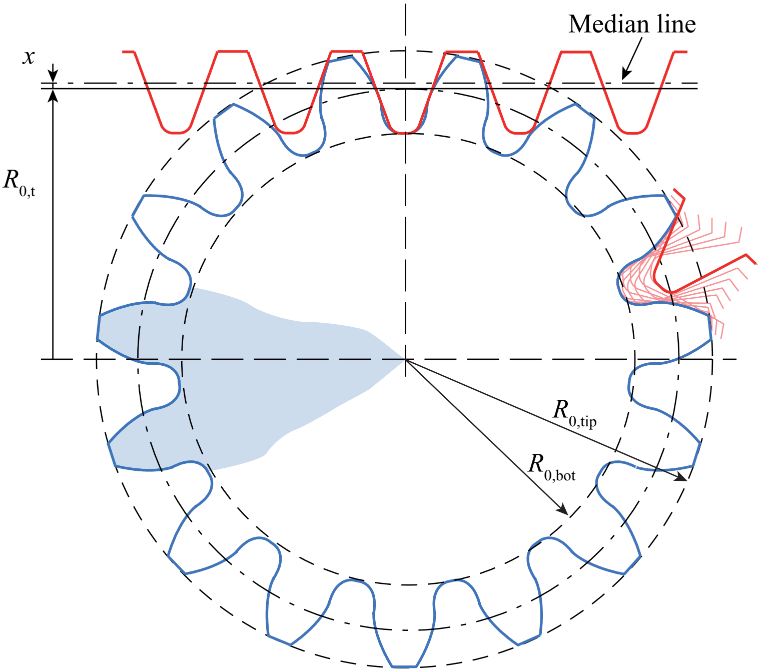

Figure 2.6: Gear in contact with basic rack. Transverse plane view.

2.2 Helical Gear Geometry

Besides that the gear tooth profile should be conjugated to the basic rack, basic gear parameters are needed to define the complete gear wheel. These parameters are the gear tooth number z, the addendum modification xm_{n}, and the gear face width b.

The normal section of the basic rack is described by Vedmar [7] using the coordinates ξ_{n} and η_{n}, see Fig. 2.2 and Fig. 2.4. The coordinate ξ_{n} is strictly increasing in the interval $-\pi/2 \leq \xi_{\mathrm{n}} \leq \pi/2$, therefore ξ_{n} can be chosen as a unique parameter to describe the complete basic rack profile, i.e. $\eta_{\mathrm{n}} = \eta_{\mathrm{n}}(\xi_{\mathrm{n}})$. This is true for the rack with and without modifications. To have only one unique parameter to describe the basic rack is very convenient in the future calculations.

The gear tooth has involute profile in, and only in, the transverse plane, and in this plane the basic rack coordinates are

$$\begin{aligned} \xi_{\mathrm{t}} &= \frac{\xi_{\mathrm{n}}}{\cos\beta} \\ \eta_{\mathrm{t}} &= \eta_{\mathrm{n}} \end{aligned} \tag{2.1}$$

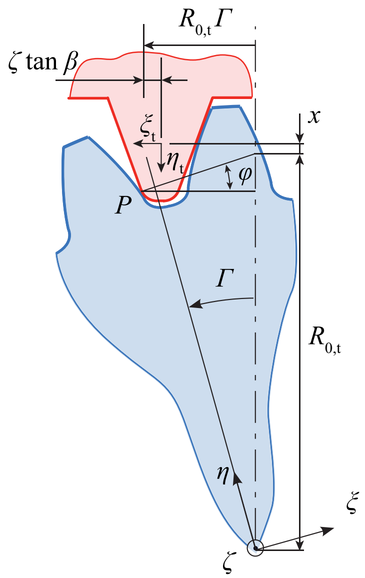

Figure 2.7: Gear in contact with basic rack at point P. Transverse plane view.

Presupposing a gear blank with the outer diameter $2R_{\text{tip}}$, the complete gear geometry is found by rolling the basic rack profile over the gear reference radius $R_{\text{t}} = R_{0,\text{t}} m_{\text{n}} = m_{\text{n}} z/2/\cos\beta$, see Fig. 2.6. In Fig. 2.7, the basic rack is in contact with the gear at point P. Dividing with the normal module m_{n}, the non-dimensional coordinates describing the complete conjugate gear tooth surface are

$$\mathbf{r}\left(\xi_{\text{n}},\zeta\right) = \begin{pmatrix} \xi\left(\xi_{\text{n}},\zeta\right) \\ \eta\left(\xi_{\text{n}},\zeta\right) \\ \zeta \end{pmatrix} = \begin{pmatrix} R_{0,\text{t}}\sin\Gamma - \dfrac{\eta_{\text{n}}-x}{\sin\varphi}\cos(\Gamma-\varphi) \\ R_{0,\text{t}}\cos\Gamma + \dfrac{\eta_{\text{n}}-x}{\sin\varphi}\sin(\Gamma-\varphi) \\ \zeta \end{pmatrix} \tag{2.2}$$

where $-b_0/2 \leq \zeta \leq b_0/2$, and $\eta(\xi_{\text{n}},0)$ divides the tooth space in two equal symmetric parts. Here, the slope of the rack profile is

$$\cot(\varphi) = -\frac{d\eta_{\text{t}}}{d\xi_{\text{t}}} = -\frac{d\eta_{\text{n}}}{d\xi_{\text{n}}}\cos\beta \tag{2.3}$$

The contact normal must always be directed through the pitch point, which gives the relation

$$\Gamma(\xi_{\mathrm{n}},\zeta) = \frac{-\dfrac{\xi_{\mathrm{n}}}{\cos\beta} + (\eta_{\mathrm{n}} - x)\cot\varphi + \zeta\tan\beta}{R_{0,\mathrm{t}}} \tag{2.4}$$

The spur gear geometry is found by setting $\beta = 0$ in Eq. 2.1, 2.3, and 2.4.

Chapter 3

Gear Manufacture

There are several methods to manufacture involute helical gears. Figure 3.1 displays the most commonly used in industry. The choice of manufacturing method depends on the gear wheel design, gear wheel size, accuracy, production quantity, machines available, application, and so forth. This work is limited to material removal manufacturing methods, hobbing, shaping, and gear form milling in particular. Material removal methods are usually divided into generating and form copying methods, where the corresponding tools can be used for roughening (R), semi-finishing (SF), and finishing (F) operations.

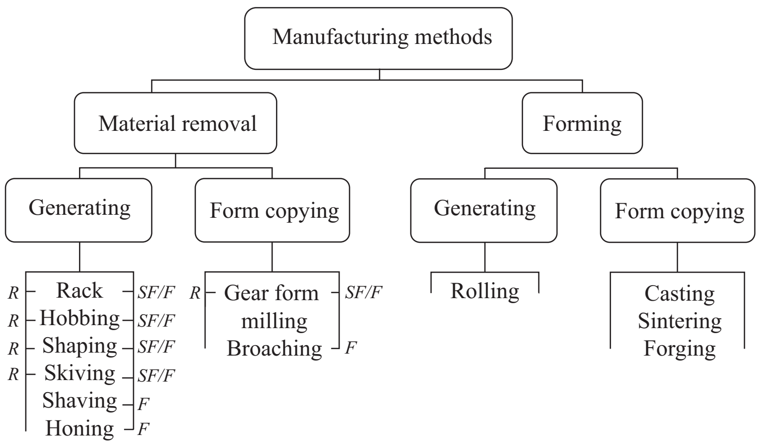

Figure 3.1: Most common gear manufacturing methods used in industry. R: roughening, SF: semi-finishing, and F: finishing

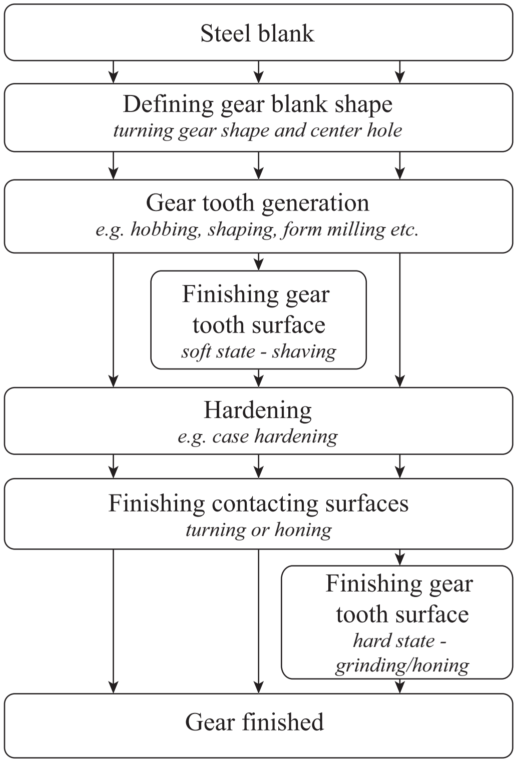

Figure 3.2: Gear manufacturing process steps [8].

The production flow is similar for gear wheels manufactured in material removal operations. Figure 3.2 shows the outline of the production flow [8]. This figure displays three choices of production paths. One alternative is to cut the gear teeth without finishing operation. This production path is, however, not suitable for high accurate gearing or for high performance gears. The normal situation is to rough cut the gear teeth prior to a finishing operation. If the gear teeth are cut in a pre-shave milling operation, the teeth are refined in a soft state by a shaving operation prior to hardening, such as case hardening. Further refinement of the tooth surface is not proceeded. There is, however, the risk that the tooth distorts after the hardening stage using this production path. The distortion can, to some degree, be compensated for in advance in order to minimize the geometrical errors. Alternatively, the gear tooth surface is refined after hardening, using grinding or honing tools. In this case, the tooth surface is resurfaced in the final production step, giving the best surface finish, profile and gear wheel accuracy.

3.1 Tool Geometry and Kinematics

Gear cutting tools are usually classified in generating tools and form copying tools as shown in Fig. 3.1. The advantage of generating tools is that they work under conjugate action, thereby the tools are universal and able to cut a wide range of gear teeth and helical angles. The cutting edge geometry of form copying tools are instead a direct copy of the gear tooth gap to shape. These tools are, on the other hand, not universal; they must be designed for each gear tooth geometry to cut.

Using such tools as hobs or form wheels, the general principles are the same regardless if the work piece is cut in a milling process or the cut tooth space is ground in a refining process. The main difference, besides process parameters, is that the milling tools have defined cutting edges that remove material, whereas grinding tools remove material by fine abrasive grains.

This chapter discusses the tool geometry and process related topics.

3.1.1 Generating Tools

Hob

If it is a threaded tool, it is in this work considered to be a hob. Regardless if the tool is a milling or a grinding tool, where a grinding hob is also referred to as a grinding worm.

To manufacture the designed gear tooth correctly, the hob should be conjugate to the same basic rack as the gear. It is in this respect faulty to consider the hob tooth profile to agree with the normal section of the rack profile, or to be a series of rack cutters. In some occasions this approximation is used for small lead angle hobs. The hob should, however, be considered as a helical gear [9], and the tooth profile will by this be slightly curved.

The hob has one tooth to a few teeth g - normally named entrances, starts, or threads, and a very large helical angle β - often the complementary lead angle λ is used. To make the hob an efficient cutting tool, the hob thread is gashed to provide cutting teeth. These cutting teeth are assumed plane, and orientated in an arbitrary direction. The normal direction to the plane of the cutting tooth is defined by

$$\mathbf{n}_\mathrm{s} = (n_{\mathrm{s},\xi}, n_{\mathrm{s},\eta}, n_{\mathrm{s},\zeta}) = (\cos\gamma \sin\kappa, \quad \sin\gamma, \quad \cos\gamma\cos\kappa) \tag{3.1}$$

where γ is the hook angle and κ is the gash angle. With this orientation of the cutting plane, the cutting edge is found by the cutting plane intersection with the hob thread profile [7, 10]. To make the resharpening of high speed steel hobs easier, the gash angle usually coincides with the hob lead angle, $\kappa = \lambda$, and the hook angle $\gamma = 0$. Indexable insert hobs are not resharpened so these angles can, at least in theory, be chosen more freely to for example optimize chip removal. Further, the cutting teeth are assumed to have sufficient tooth relief to avoid interference in the milling process. After the hob is gashed, it will have the total of N cutting teeth with n cutting teeth per hob revolution.

To cut the gear, the hob is positioned at the center distance $a = R_{\mathrm{h,t}} + x_{\mathrm{h}} m_{\mathrm{n}} + R_{\mathrm{g,t}} + x_{\mathrm{g}} m_{\mathrm{n}}$ to the gear axis, and the hob axis at the cross angle $\lambda + \beta$ with respect to the gear axis. The gear can be machined in either climb milling or conventional milling depending on the direction of the feed, see Fig. 3.3. The feed rate is defined as S, the distance the hob travels in the gear axial direction per gear revolution. Simultaneously the hob and the gear rotates in a timed relation

$$g\dot{\phi} = z\dot{\psi} \tag{3.2}$$

The load on each cutting tooth vary heavily in hobbing. The hob length l_{h} must be sufficient, so that the hob's cutting teeth in the outer regions of

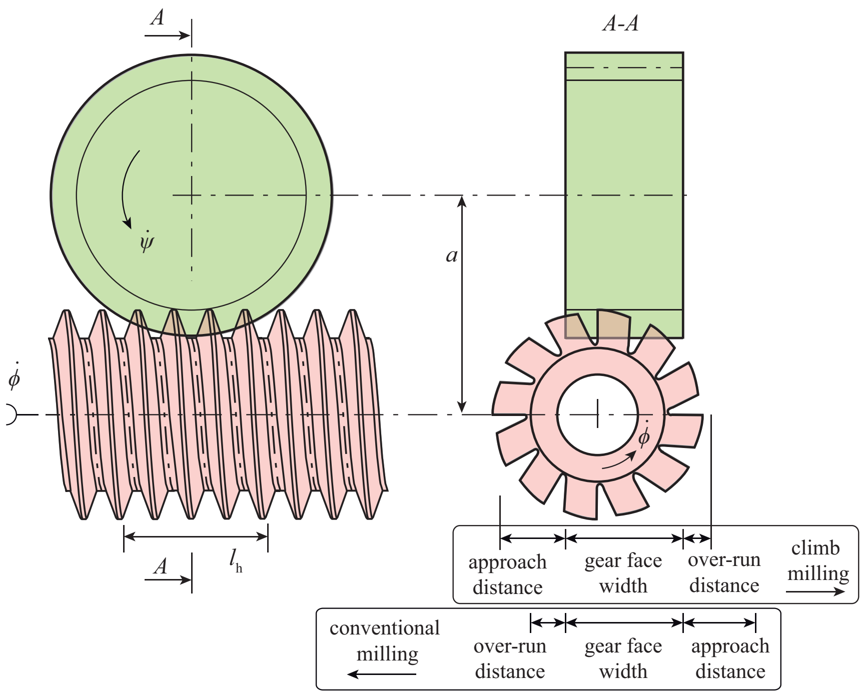

Figure 3.3: Gear cut by a hob.

the generating zone do not have to withstand increased load. Modern hobs are normally longer than this requirement. Longer hobs are used as it is possible to spread the point of maximum load, normally by using tangential shift strategies, to try to even the wear distribution and as a consequence increase the tool life. Additionally, hobs can also be combined by essentially two hobs, where one half is for roughing cut and the other half, normally of a very high quality class, is performing the semi-finishing or the finishing cut.

Multiple start hobs are used to increase productivity, as these allow higher rotation speeds of the work piece than using single start hobs. The productivity gain is not linear as Eq. 3.2 indicates, because multiple start hobs are usually diametrically larger

$$R_{\mathrm{h,tip}} = m_{\mathrm{n}} \left(\frac{g}{2 \sin \lambda} + x + h_{0,\mathrm{t}} \right) \tag{3.3}$$

which lead to increased approach and over-run distances, see Fig. 3.3. Additionally, to maintain reasonable cutting speed the hob rotational speed is lower, and the feed rate is lower compared to single start hobs to reduce the load on the cutting teeth. As a rule of thumb, Endoy [4] states that the productivity is increased by 60 % for two-start, 90 % for three-start, and 120 % for four-start hobs compared to single start hobs.

Additional consideration should be regarded when using multiple start hobs. Since the hob threads are ground in separate operations, each thread has its own specific manufacturing errors. These possible errors will be reproduced on the cut gear. If the gear tooth number is divisible with the number of entrances of the hob, the gear is cut with good profile accuracy but pitch errors will be present. The common practice is to instead choose a hob where the number of starts are not divisible with the gear tooth number. The hob error is then spread out on all gear teeth, good pitch accuracy is achieved, however, to the cost of rougher surfaces on the gear tooth flanks. Subsequent refining, such as honing, grinding, or shaving will address the profile accuracy.

Single start hobs and multiple start hobs are normally measured in industry to control for possible geometrical tool errors. A total of 17 standardized individual and cumulative deviations have to be inspected in order to assess a hob completely [11]. The hob measurements are performed in a specialized measurement instrument, where a detailed description of these measurements are outlined in VDI/VDE 2606 - "Measurement of gearing tools - measuring of hobs" [12]. Based on these measurements, the hob is categorized in the hob quality classes AA, A, B, C, and D according to DIN 3968 [13], where the AA quality class is the most accurate hob geometry.

Shaper cutter

The shaper cutter is the most versatile cutting tool working under conjugate action. Hobs and rack cutters are, by geometrical restrictions, unable to cut internal gears. The same shaper cutter can, however, cut an internal gear, an external gear, or a rack, see Fig. 3.4. Moreover, the shaper cutter is able to cut gear teeth adjacent to shoulders, cluster gears, and herringbone gears, due to the small over-run in the cutting stroke.

The shaper cutter closely resembles the external gear, but has an increased addenda and a rounded tooth tip. The rounded tool tip is said to increase the tool life, as a sharp corner is easily worn, and to increase the strength of the cut gear [14]. In the literature, this rounded tool tip is a circular sector in the transverse plane [15, 16, 17, 18]. To cut the intended gear geometry, the tool and the gear should share a mutual basic rack. There is, however, a risk that the tooth tip can be undercut, and an undercut tool will not produce the correct gear fillet. As derived in paper V, the shaper cutter can be conjugate to the basic rack with circular fillet, however, very large tooth numbers are needed to avoid an undercut tool. These large tooth numbers are impractical

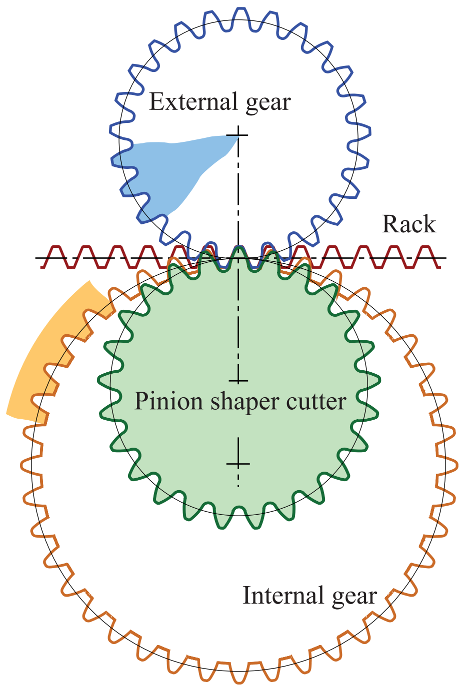

Figure 3.4: Pinion shaper cutter cuts an internal gear, an external gear, or a rack.

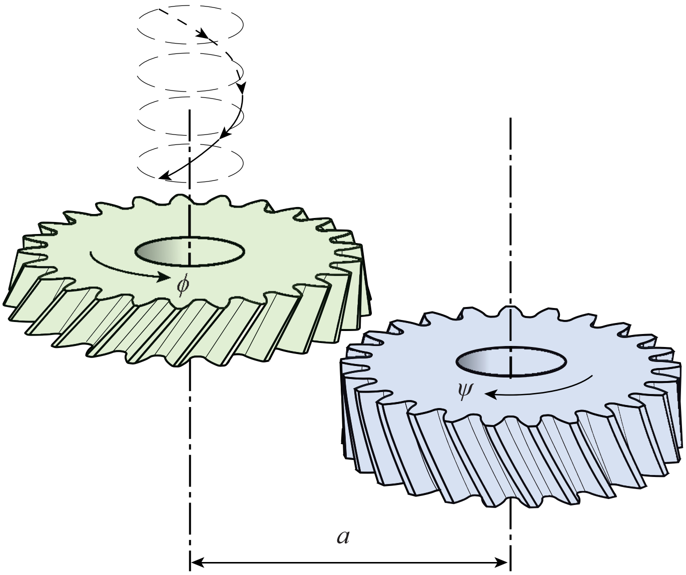

Figure 3.5: Helical gear cut by a shaper cutter.

for industrial use. In paper V it is shown that the cutter with a circular tip rounding is, at least very closely, conjugate to a basic rack with an elliptical fillet. If this modification is made to the basic rack profile, it is shown that the tool can have substantially fewer teeth without this type of undercut. This cutter will, however, cut a fillet different from the fillet defined by the basic rack with a circular fillet.

To cut the gear, the shaper cutter is positioned at the center distance $a = R_{\mathrm{g,t}} + x_{\mathrm{g}} m_{\mathrm{n}} \pm R_{\mathrm{s,t}} \pm x_{\mathrm{s}} m_{\mathrm{n}}$, where the upper sign is for external gears and lower sign is for internal gears. The gear and shaper cutter axes are here considered to be parallel, and the sum of the addendum corrections must then be equal to zero, i.e. $x_{\mathrm{g}} \pm x_{\mathrm{s}} = 0$, to cut the correct gear geometry.

The shaper cutter cuts the gear only in the forward stroke in a reciprocating manner. On the return stroke the cutter is retracted to avoid interference. During this cutting action the gear wheel is indexed by continuous revolution, and this indexing motion equals to the rotary feed. If helical gear teeth are machined, a helical guide is used. Whilst the shaper spindle reciprocates, the helical guide provides a helical motion superimposed to the shaper rotation, see Fig. 3.5.

3.1.2 Form Copying Tools

Form milling Cutter

The form milling cutter is a disc type tool, which is formed to the tooth space to cut. For spur gears, the cutting edge geometry is a direct copy of the tooth space to cut, hence a form copying tool. This tool can not cut arbitrary gear tooth numbers. The form milling cutter must be designed for the gear geometry to cut, which means that the gear and the cutter must share design parameters such as the gear tooth number, the addendum correction factor, etc..

A series of standard cutters do exist for cutting spur gears, where each cutter cuts a range of gear tooth numbers [19]. The cutter is designed for the lowest number in the range, and gears with higher tooth numbers are cut with a slight profile error. Sometimes, helical gears are cut by spur gear cutters, by matching the cutter to the virtual-spur tooth number. However, to cut helical gears correctly, the form milling cutter must be conjugate to the gear tooth space to cut. The form milling cutter is not considered as a generating tool, perhaps, as it is only conjugate to the tooth space of the gear to cut and not to the basic rack profile. The design methodology presented in paper IV and VI, can be used to determine the geometry of both spur and helical gear cutters.

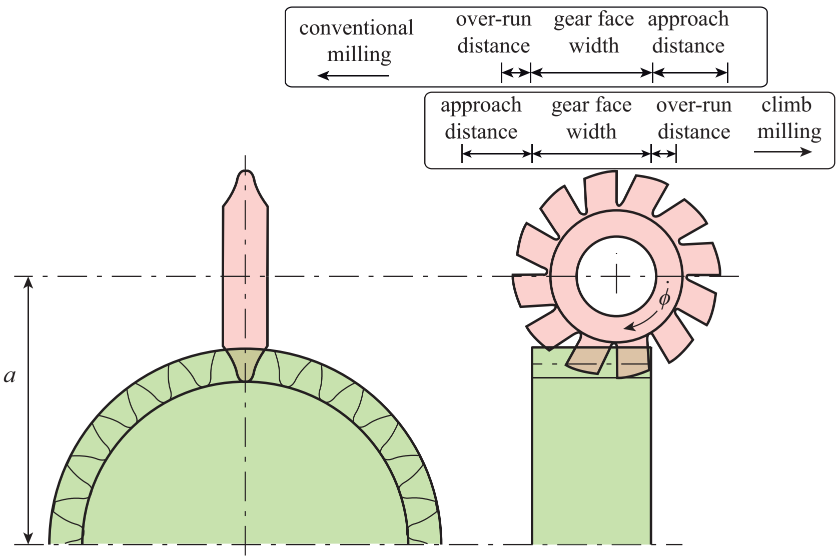

Figure 3.6: Gear cut by a form milling cutter.

The form milling cutter is positioned at the center distance a and the tool rotational axis at the angle β_{c} to the gear transverse plane, in order to cut the gear. It is not evident how the angle β_{c} should be chosen since the helical angle varies with the radius according to the relation $r_{\mathrm{i}} \cot \beta_{\mathrm{i}} = \text{constant}$, on the helical gear tooth flank. It can, however, be used so that the angle β_{c} coincides with the helical angle β_{t} of the gear at the reference radius R_{t}. The form wheel can also be positioned at another angle $\beta_{\mathrm{c}} \neq \beta_{\mathrm{t}}$, at least if the angle β_{c} corresponds to a helical angle on the gear tooth radius. However, the geometry of the form wheel must be determined at the same angle as β_{c} to machine the helical profile correctly.

The milling cutter is gashed to provide the cutter with n cutting teeth, separated by the angular increment $\Delta\phi = 2\pi/n$. The cutting teeth are provided with sufficient tip and side relief to avoid interference in the milling process.

As for hobbing, the form milling cutter can machine the gear in climb or conventional milling, see Fig. 3.6. The feed rate S is defined as the distance the milling cutter travels per cutter revolution in the gear axis direction, alternatively the feed rate is defined as the distance traveled per cutting tooth i.e. $s = S/n$. After one tooth space is cut, the next tooth space is indexed by the machines indexing mechanism. Thereby, possible pitch errors are caused by the accuracy of the indexing mechanism, whereas profile errors are due to the milling cutter and its feed.

3.2 Gear Tooth Surface Topography

The tools described in the previous section will, in theory, cut the ideal gear tooth profile. However, the machined gear tooth surface will have errors by the finite number of cuts in combination with the feed. Additional manufacturing errors will be present if the gear is cut in industrial conditions, where geometrical errors connected to the tool and the machine will directly affect the machined gear tooth surface.

In all of the production paths mentioned in Fig. 3.2, it is of highest importance to achieve a controlled surface topography. Especially, if the gear tooth is finished cut, as this surface will be the final tooth geometry the gear will have in operation. If the gear tooth will be refined in subsequent operation, it is also of importance to in advance be able to predict the surface topography. If tool and machine related errors are small enough to neglect, it would be possible to chose optimal process parameters so that the gear tooth surface meet the pre-specified requirements.

If tool and machining errors are significant, these errors will affect the machined tooth surface topography. If these errors can be detected, it would be possible to improve the manufacturing process. It is, however, hard to link possible manufacturing errors to the cut gear tooth surface. To be able to find how these errors affect the cut surface, isolated or combined, mathematical models are developed in order to calculate the cut tooth surface where these process related errors are introduced. It would be possible to identify error sources and to quantify their impact on the cut tooth surface using these models. This gives the possibility to in a systematic manner identify the error sources that affect the gear quality in the most negative way. This capability opens up for improvement possibilities, to for example tighten the production and the tool related tolerances that affect the gear quality the most.

The material removal is far easier in the milling operation than in the refining operations. If the gear teeth can be machined to tight tolerances in a controlled way, it would definitely make the finishing steps easier, such as shaving, grinding, and honing operations. Most important, however, is that the gear tooth profile is produced within tolerances at final inspection. A lot of value is put into the gear wheel by the production steps. If the gears are not produced within tolerances they will be discarded when they are close to their highest value.

Most of the previous published research have focused on predicting cut tooth surface topography after hobbing, and not after form milling or shaping. Different CAD-packages have been developed in order to predict the hobbed gear tooth surface, for example the works presented by Michalski and Skoczylas [20] and Bergseth [21]. In Bergseth's work small damages to the cutting tooth were made, by small geometrical notches on the cutting edge, to imitate a worn hob when modeling the hobbed tooth surface. In both mentioned works, gear blank material is logically removed if interference occur when the cutting edge makes its path through the work piece; the cut surface is determined by differences. In these CAD packages the material is not continuously removed, but instead in discrete time frames. This calculation procedure can give numerical inaccuracies.

Little work have been focused on the machined tooth surface where tool or process related errors are considered. Parallel to this work, however, Gravel presented a simulation model that incorporates tool and process related errors in gear hobbing [22].

3.2.1 Cut Surface

In order to find the cut surface, we start from the surface we aim to manufacture. The ideal smooth gear tooth surface is described by the surface conjugate to the basic rack profile in Ch. 2.2, using the parameters ξ_{n} and ζ, i.e. $\mathbf{r}(\xi_{\mathrm{n}},\zeta)$ in Eq. 2.2. This gear surface will already have possible modifications depending on the basic rack design chosen.

The tool is conjugate to the basic rack too (or in case of the form milling tool, conjugate to the tooth space). The tool geometry is described in Ch. 3.1. The tool's cutting edges will cut the gear tooth space by successive cuts. To identify the cutting edges they are numbered, where cutting edge i will cut the surface S_{i} by its path through the work piece. To describe the cut surface S_{i} two parameters are needed, one parameter $\xi_{\mathrm{n,c}}$ along the tool cutting edge and one parameter ϕ for the position of the tool relative the work piece (in this case the total tool rotational angle). The surface cut by the tool is described in the same coordinate system as the gear wheel. The distance h_0 from a point $\mathbf{r}(\xi_{\mathrm{n}},\zeta)$ on the ideal smooth surface, in its surface normal direction $\mathbf{n}(\xi_{\mathrm{n}},\zeta)$, to the surface $\mathbf{r}_{\mathrm{S_i}}(\xi_{\mathrm{n,c}},\phi)$ cut by the i : th cutting edge is found by

$$\mathbf{r}(\xi_{\mathrm{n}},\zeta) - h_0 \frac{\mathbf{n}(\xi_{\mathrm{n}},\zeta)}{|\mathbf{n}|} = \mathbf{r}_{\mathrm{S_i}}(\xi_{\mathrm{n,c}},\phi) \tag{3.4}$$

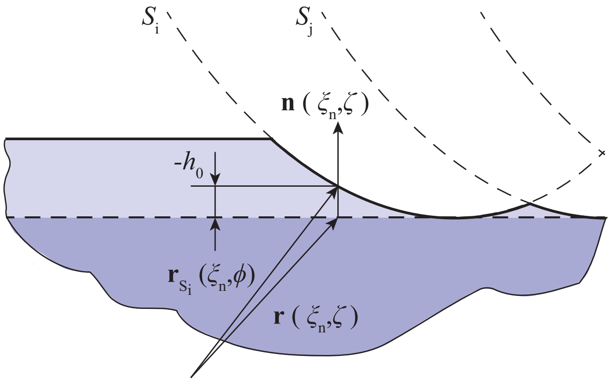

Figure 3.7: Determine the cut gear tooth surface topography.

see Fig. 3.7. Here, the surface normal of the ideal smooth tooth surface is given by

$$\mathbf{n}(\xi_{\mathrm{n}},\zeta) = \begin{pmatrix} n_\xi \\ n_\eta \\ n_\zeta \end{pmatrix} = \frac{\partial \mathbf{r}}{\partial \xi_{\mathrm{n}}} \times \frac{\partial \mathbf{r}}{\partial \zeta} = \begin{vmatrix} \hat{\xi} & \hat{\eta} & \hat{\zeta} \\ \frac{\partial \xi}{\partial \xi_{\mathrm{n}}} & \frac{\partial \eta}{\partial \xi_{\mathrm{n}}} & \frac{\partial \zeta}{\partial \xi_{\mathrm{n}}} \\ \frac{\partial \xi}{\partial \zeta} & \frac{\partial \eta}{\partial \zeta} & \frac{\partial \zeta}{\partial \zeta} \end{vmatrix} \tag{3.5}$$

Equation 3.4 can be solved using Newton-Raphson's method. In component form this equation is expressed as

$$\begin{aligned} f_\xi(\xi_{\mathrm{n,c}},\phi,h_0) &= \xi_{\mathrm{S_i}}(\xi_{\mathrm{n,c}},\phi) + h_0\frac{n_\xi(\xi_{\mathrm{n}},\zeta)}{|\mathbf{n}|} - \xi(\xi_{\mathrm{n}},\zeta) = 0 \\ f_\eta(\xi_{\mathrm{n,c}},\phi,h_0) &= \eta_{\mathrm{S_i}}(\xi_{\mathrm{n,c}},\phi) + h_0\frac{n_\eta(\xi_{\mathrm{n}},\zeta)}{|\mathbf{n}|} - \eta(\xi_{\mathrm{n}},\zeta) = 0 \\ f_\zeta(\xi_{\mathrm{n,c}},\phi,h_0) &= \zeta_{\mathrm{S_i}}(\xi_{\mathrm{n,c}},\phi) + h_0\frac{n_\zeta(\xi_{\mathrm{n}},\zeta)}{|\mathbf{n}|} - \zeta(\xi_{\mathrm{n}},\zeta) = 0 \end{aligned} \tag{3.6}$$

These equations contain three unknowns. Besides the distance $h = h_0 m_{\mathrm{n}}$ from the ideal smooth tooth surface to the cut surface, also the position along the cutting edge ($\xi_{\mathrm{n,c}}$) and the rotational angle of the tool (ϕ) are unknowns. In matrix format, a solution can be found by

$$\begin{pmatrix} \xi_{\mathrm{n,c,k+1}} \\ \phi_{\mathrm{k+1}} \\ h_{0,\mathrm{k+1}} \end{pmatrix} = \begin{pmatrix} \xi_{\mathrm{n,c,k}} \\ \phi_{\mathrm{k}} \\ h_{0,\mathrm{k}} \end{pmatrix} - \mathbf{M}^{-1} \begin{pmatrix} f_\xi(\xi_{\mathrm{n,c,k}},\phi_{\mathrm{k}},h_{0,\mathrm{k}}) \\ f_\eta(\xi_{\mathrm{n,c,k}},\phi_{\mathrm{k}},h_{0,\mathrm{k}}) \\ f_\zeta(\xi_{\mathrm{n,c,k}},\phi_{\mathrm{k}},h_{0,\mathrm{k}}) \end{pmatrix} \tag{3.7}$$

where

$$\mathbf{M} = \begin{pmatrix} \dfrac{\partial f_\xi}{\partial \xi_{\mathrm{n,c}}} & \dfrac{\partial f_\xi}{\partial \phi} & \dfrac{\partial f_\xi}{\partial h_0} \\ \dfrac{\partial f_\eta}{\partial \xi_{\mathrm{n,c}}} & \dfrac{\partial f_\eta}{\partial \phi} & \dfrac{\partial f_\eta}{\partial h_0} \\ \dfrac{\partial f_\zeta}{\partial \xi_{\mathrm{n,c}}} & \dfrac{\partial f_\zeta}{\partial \phi} & \dfrac{\partial f_\zeta}{\partial h_0} \end{pmatrix} = \begin{pmatrix} \dfrac{\partial \xi_{\mathrm{S_i}}}{\partial \xi_{\mathrm{n,c}}} & \dfrac{\partial \xi_{\mathrm{S_i}}}{\partial \phi} & \dfrac{n_\xi}{|\mathbf{n}|} \\ \dfrac{\partial \eta_{\mathrm{S_i}}}{\partial \xi_{\mathrm{n,c}}} & \dfrac{\partial \eta_{\mathrm{S_i}}}{\partial \phi} & \dfrac{n_\eta}{|\mathbf{n}|} \\ \dfrac{\partial \zeta_{\mathrm{S_i}}}{\partial \xi_{\mathrm{n,c}}} & \dfrac{\partial \zeta_{\mathrm{S_i}}}{\partial \phi} & \dfrac{n_\zeta}{|\mathbf{n}|} \end{pmatrix} \tag{3.8}$$

This calculation method will determine the unknown parameters h_0, $\xi_{\mathrm{n,c}}$ and ϕ using analytically differentiable functions, thus, a convergent solution will especially give the distance $h = h_0 m_{\mathrm{n}}$ directly without further numerical approximations.

The machined tooth surface is found by repeating this calculation procedure and considering all paths made by the tool. To ensure a fast calculation scheme, only the surfaces cut nearby the point considered on the ideal surface need to be calculated, see Fig. 3.7. Figure 3.8, 3.9, and 3.10 shows examples of the calculated tooth surface topography of spur and helical gears cut by a hob, a form milling cutter, and shaper/rack cutter respectively. In these figures the complete tooth surface, including the fillet, is mapped to a plane surface. A wavy pattern is present in each of these surfaces, and in the valleys of this wavy pattern the cut tooth surface agrees with the ideal smooth tooth surface. It should be noted that the deviations are magnified to a scale very large compared to the scale in the tooth height and the tooth width directions.

The surface topography of the hobbed and the form milled tooth surfaces are visually quite similar, however, the surfaces are generated very differently. The hob, without cutting teeth, is a helical gear, and two helical gears mounted on crossed axis will have a point contact. The hob cutting tooth will remove material in the proximity of this imaginary contact point. By the finite number of cuts, due to the finite number of cutting teeth, the cut surface will have a wavy pattern in the tooth height direction, see Fig. 3.8. The distance between the valleys in the width direction equals the feed S, which is the distance the hob travels until the same gear tooth space reapers in the generating zone. In contrast, the distance between the valleys of the form milled gear tooth surface equals the distance s, the cutter feed distance per cutting tooth. Each valley is shaped by one single cutting edge in one cut, thus a wavy pattern in the tooth height directions is not present.

A gear machined by a grinding hob will not have the wavy pattern in the tooth height direction. The grinding hob does not have any defined cutting teeth, the material is removed by very fine grains of abrasive material. A milling hob with sufficient many cutting teeth can imitate a grinding hob.

The wavy pattern in the tooth height direction will vanish if the number of cutting teeth are enough. A hob with many cutting teeth is used in the analysis performed in paper III, where the gear is refined in a hob grinding operation. The wavy pattern in the tooth width direction will, however, be present for both milled and ground surfaces machined by a hob.

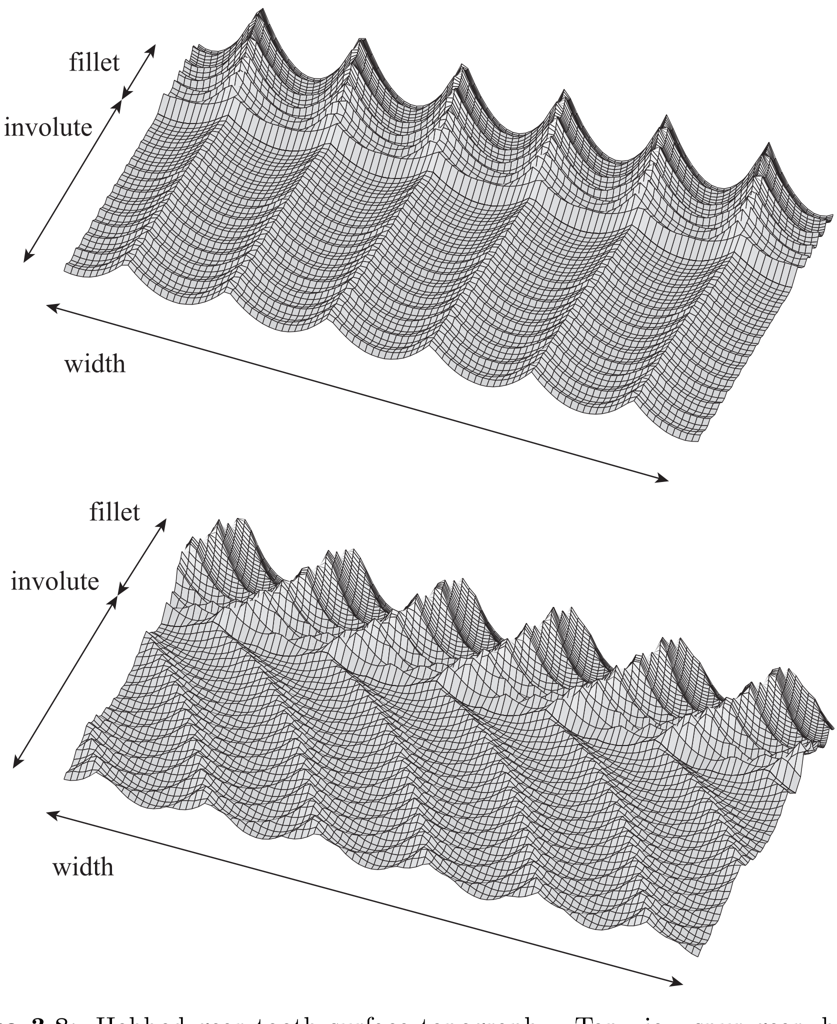

Figure 3.8: Hobbed gear tooth surface topography. Top view spur gear, bottom view helical gear.

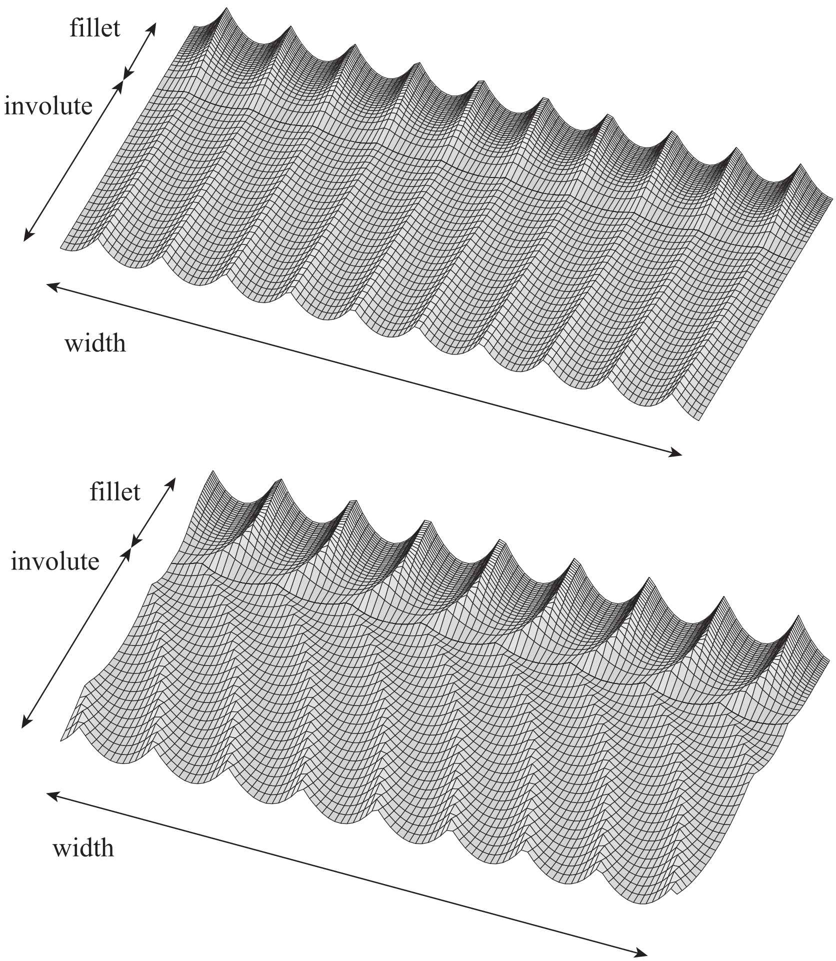

Figure 3.9: Form milled gear tooth surface topography. Top view spur gear, bottom view helical gear.

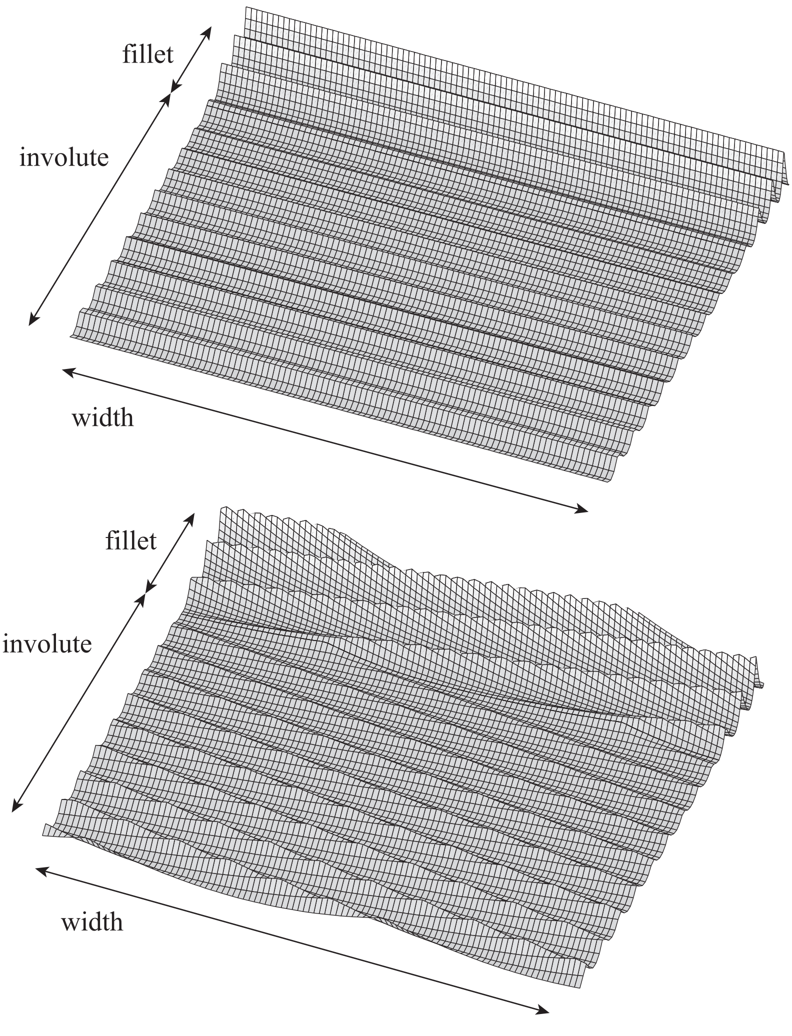

Figure 3.10: Shaper cut gear tooth surface topography. Top view spur gear, bottom view helical gear.

When gears are cut in industrial conditions it is likely that tool and machine related errors are present. These possible errors will result in additional errors on the cut gear tooth surface. Tool and manufacturing related errors are considered in paper I, II, and III for gear hobbing and in paper IV for gear form milling. For a specific description of the error sources considered in the machining operations the reader is referred to these papers. The error sources will, however, affect the cutting edge path and is included in the description of $\mathbf{r}_{S_i}$ in Eq. 3.4.

As mentioned in Ch. 2.1, protuberance tools are used to acquire additional material on the tooth flanks. This is a machining allowance, alternatively expressed as a grinding stock, and this thin slice of additional material on the tooth flank is about 0.1 mm thick. The protuberance tool also intentionally undercut the gear tooth in order to ensure a controlled transition between the involute and the fillet region. This undercut is performed as only the material in the involute region will be removed by grinding, shaving, or honing operations, whereas the fillet region will be unchanged.

The grinding stock should be sufficient to swallow the manufacturing errors, so that the final tooth surface is not impaired after the grinding stock is removed in the finishing operation. In paper II it is studied what gear quality is achieved after milling, cut by different hob quality classes and feed rates. The minimum amount of grinding stock needed to ensure that the final tooth surface is not affected by the roughening cut is also predicted for each hob quality class at various feed rates. Figure 3.11 shows the cut tooth surface by a hob with protuberance, using an ideal hob geometry and using a quality class B hob.

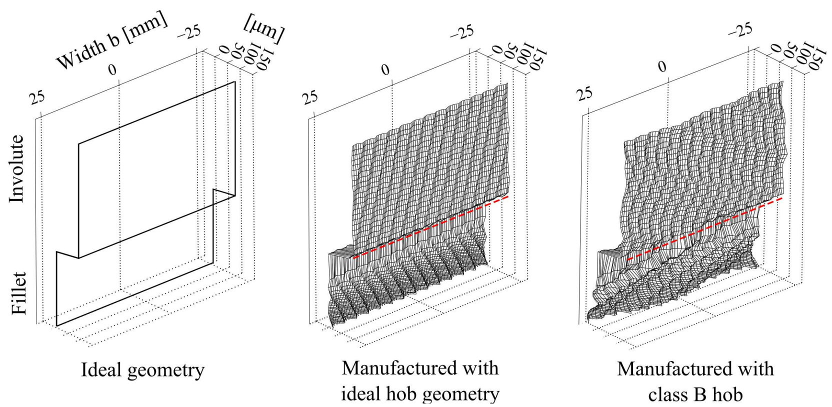

Figure 3.11: Helical gear tooth surface topography hobbed by an ideal hob geometry and a class B hob, from paper II.

3.2.2 Gear Tooth Deviations

Control measurements are carried out to inspect the gear quality, where the gear wheel is measured on a dedicated CNC (computer numerical control) measuring center. The results from these measurements include tooth surface errors, pitch errors, eccentricity etc.. In this thesis, the focus is on the tooth surface errors.

The measurements are carried out both before and after the final finishing operation. The gear tooth surface is inspected after the roughening cut, in the pre-finishing state, where it is desired that the tooth form, along the profile and the lead, should be within close accuracy. This is to ensure that the correct profile is cut, and to make the refining steps easier. The refining tool, like honing, grinding, or shaving, should ideally only remove the feed marks, and not reshape the gear tooth profile. Smaller modifications, such as tip relief, are however fabricated in the refining steps. Inspection after the final refining step is to ensure the gear tooth is produced within pre-specified tolerances.

These measurements are also the basis for the gear quality classification according to DIN 3962 part 1 and part 2 [23, 24]. The measured deviations include total error, form error, and alignment error over the tooth height and along the face width, and lead crowning and tip relief, see Tab. 3.1. Different standards are used depending on geographical or industrial affiliation, see for example DIN, AGMA, ISO, and VOLVO Group Standard. The definitions in these standards are very similar and in several cases the same. In this thesis the definitions according to Volvo Group STD 5082,81 [25] are used.

The normal procedure is to inspect four gear teeth that are evenly spaced around the gear wheel, where each tooth is measured on the right and left flank respectively. Only the tooth flank is controlled by these measurements, not the fillet. A stylus tracks the tooth surface at designated lines, over the tooth

Table 3.1: Gear tooth deviations

	Profile	Lead
Total	F_α	F_β
Alignment	$f_{\mathrm{g},\alpha}$	$f_{\mathrm{H},\beta}$
Form	$f_{\mathrm{f},\alpha}$	$f_{\mathrm{f},\beta}$
Crowning	—	c_β
Tip relief	c_a	—

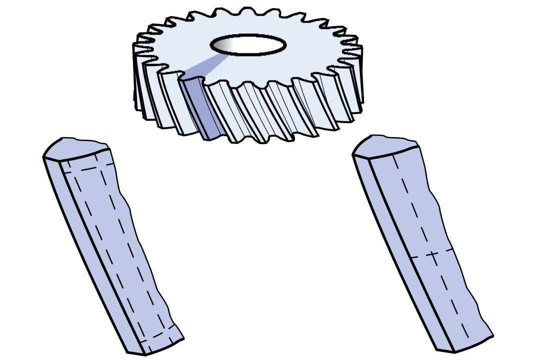

Figure 3.12: Square and cross measurement of gear tooth profile.

height at a constant width position, and along the tooth width at a constant radius. Figure 3.12 shows the two measurement schemes that usually are used in industry, alternatively they can also be combined.

Figure 3.13 shows the measuring procedure over the gear tooth height. The stylus measures the surface compared to the ideal designed tooth surface. The gear wheel rotates, while the stylus moves the rolled distance s. For the radial position r the rolled distance s is

$$s = \sqrt{r^2 - r_\mathrm{b}^2} \tag{3.9}$$

where r_b is the base circle radius. As the position of the stylus always is on the tangent line to the base circle, the deviations are measured in the normal direction of the designed tooth surface. There is, however, no absolute reference position, only relative deviations are determined.

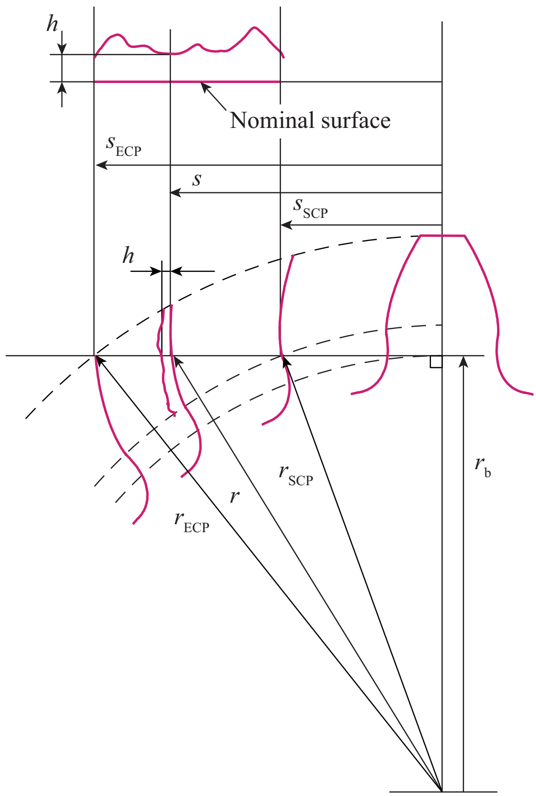

Figure 3.13: Measurement procedure of gear tooth deviations.

To inspect the profile deviations, the gear tooth is measured in the tooth height direction within the radial distance $r_{\mathrm{SCP}} < r < r_{\mathrm{ECP}}$, where "SCP" is the abbreviation for "Start Control Point" and "ECP" for "End Control Point". Alternatively, the radial distance can be expressed as the equivalent rolled distance $s_{\mathrm{SCP}} < s < s_{\mathrm{ECP}}$. Point "A" is the point where the tip relief starts. This control measurement is normally performed at a constant width position. Figure 3.14 shows the definition of the profile deviations.

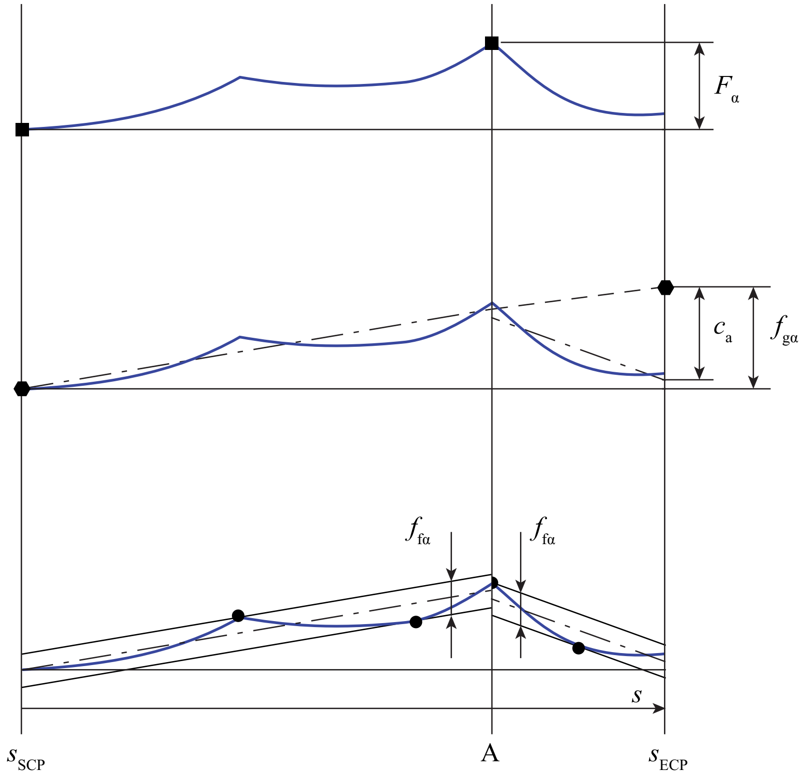

Figure 3.14: Definitions of profile deviations.

To inspect the lead deviations, the gear tooth is measured in the gear width direction at a constant radius, normally $(r_{\mathrm{SCP}} + r_{\mathrm{ECP}})/2$ unless otherwise stated. The gear tooth is evaluated within 80 % of the total face width. Figure 3.15 shows the definition of the lead deviations.

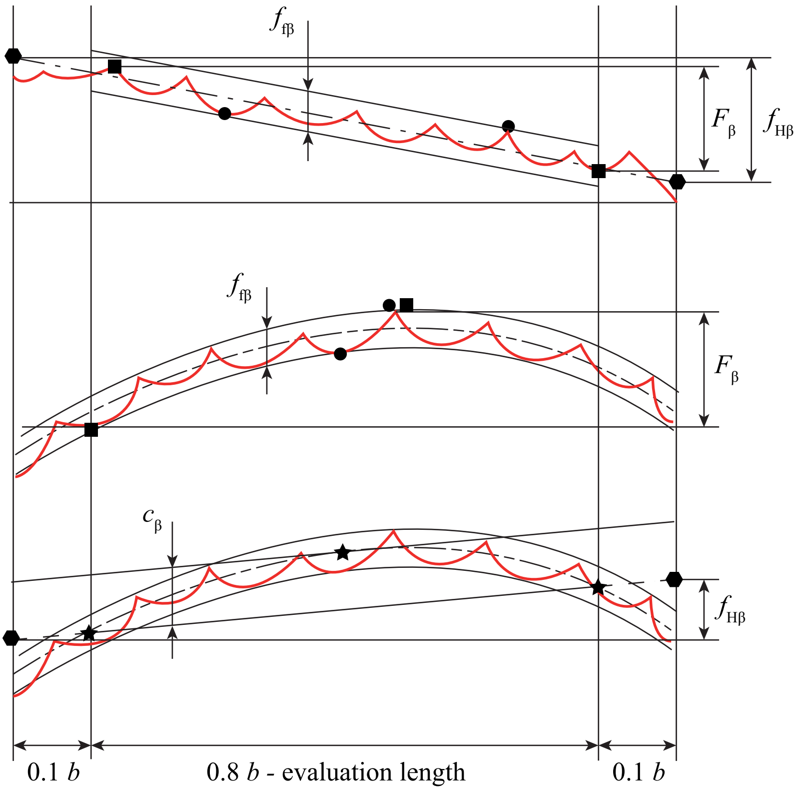

Figure 3.15: Definitions of lead deviations.

3.2.3 Gear Tooth Modifications

The gear can be manufactured with tooth modifications desired for optimum gear performance. Some are already discussed in Ch. 2.1, where these modifications are incorporated into the basic rack design.

Another common modification is to add lead crowning to the gear tooth, see Fig. 3.16. Cylindrical gears on parallel axes will have line contact if perfectly aligned, and point contact if they are not. If point contact is present by non-aligned axes, the contact will be at tooth ends where the gear teeth are most vulnerable. To avoid hard bearing at tooth ends, the gear teeth are lead crowned to center the contact [19]. This will reduce the risk of premature gear failure.

Lead crowning is designed into the tool itself for honing and shaving tools, and can be seen as a modification to the mutual basic rack of the designed gear and the tool. Lead crowning gear teeth in hobbing, shaping, and form milling, however, is accomplished by changing the machine settings in the machining operation. The center distance is changed while the tool travels over the gear face width, where the tool is plunged in at the tooth ends [19]. This results in a gear tooth where the addendum correction varies along the gear face width.

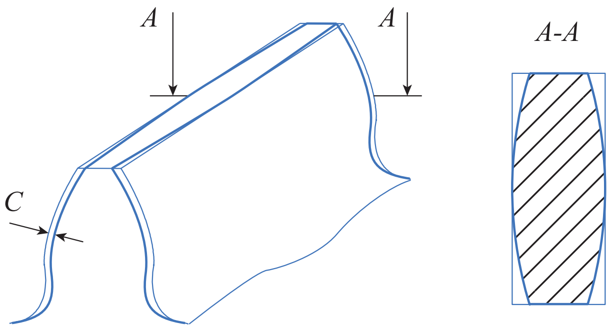

Figure 3.16: Lead crowned gear tooth.

If a milling hob or a grinding hob is used to lead crown helical gears in this way, the gear teeth will be manufactured with undesired alignment errors. This phenomena is normally called flank twist or bias errors. A gear tooth with flank twist is shown in Fig. 3.17. To measure flank twist square measurements are needed, since the alignment errors are not present in the middle of the gear tooth. That flank twist will occur is described in literature [26, 27], but no-one has previously made quantitative predictions of these alignment errors. In paper III, however, analytical equations are presented that predict the magnitude of the profile and the lead alignment errors, and in this paper an analysis explains why these alignment errors arise.

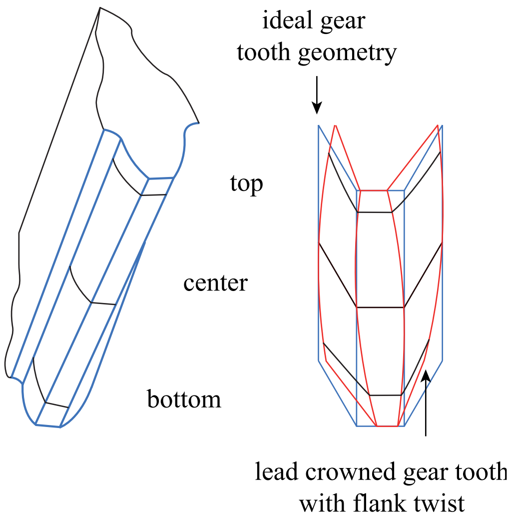

Figure 3.17: Flank twist.

3.3 Metal Cutting

A central issue in any machining operation is to be able to predict the cutting forces on the tool cutting edge. Cutting force models, which are the foundation of tool wear models, depend on mainly three parameters: chip thickness, chip width, and cutting resistance of the work piece material [28]. Therefore, an accurate determination of the chip geometry is needed.

In gear milling, the chip geometry is complex. The tool's cutting edges cut the work piece by successive cuts. The volumetric difference in between these cuts equals the undeformed chip geometry, and are confined by the cutting edges and the gear blank boundaries. A crude illustration of the chip load is presented in Dudley Gear Handbook [19], see Fig. 3.18. This figure shows that the chip area and the chip thickness along the cutting edge varies for each cut. In order to calculate the chip geometry, the cutting edge geometry and its path through the work piece have to be known.

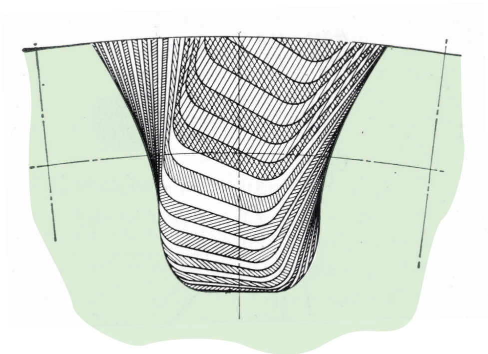

Figure 3.18: Chip loads cut by successive hob teeth [19].

Hoffmeister [29] studied the chip geometry in gear hobbing. In his work, approximate formulas are presented to determine the chip thickness and cut chip length. Hoffmeister's formula, that predicts the maximum undeformed chip thickness, is still used in industrial process planning today [30], where it is desired to limit the maximum chip thickness with consideration to the strength limit of the hob teeth. For gears of module $3 - 5\,\mathrm{mm}$, industrial empiricism suggests that the maximum chip thickness should be limited to $0.20\,\mathrm{mm} \leq h_{\max} \leq 0.25\,\mathrm{mm}$. Later, Sulzer [31] presented an extended mathematical model that determines the cut chip geometry in a hobbing process. In his work, the cutting edge geometry is approximated by the normal plane geometry of the basic rack, which geometry was described by a series of straight lines, also in the fillet section.

Different CAD-packages have been developed to determine the chip geometry and cutting forces in gear hobbing. The CAD/FEM package FRSFEM presented by Antoniadis et.al. [32] calculates the chip geometry and the cutting forces in fly hobbing, a simplified one tooth hob cutter. The pass of one tooth gap is studied, and the chip geometries and the cutting forces are considered to repeat as the hob is fed in the gear axial direction. That the chip geometries and the cutting forces repeat are, however, only true for a portion of the complete production cycle. A similar methodology is presented by Tapoglou and Antoniadis [33] in the HOB 3D CAD package, where the chip geometry is determined in three dimensions instead of planar chip description. Another example is the SPARTApro software developed at WZL Aachen [34]. More recent, Sabkhi et. al. [35] used a CAD/FEM software to calculate the cutting forces in gear hobbing. The hob was scanned in three dimensions using a Breukmann system, which was used as input to the model. The scanning error was estimated to 0.2 mm, which is very large compared to the reported maximum calculated chip thickness of 0.05 mm.

The chips are very thin, thus, an accurate geometrical method is needed to achieve satisfactory results. Determining the chip thickness by differences can give numerical inaccuracies. A method to calculate the chip thickness directly is developed by Vedmar et. al. [10], and by this method the chip thickness is directly determined by an analytical differential description to keep numerical errors to a minimum.

3.3.1 Chip Geometry

The tool cuts the gear blank by successive cuts. The chip geometries are determined by these cuts and the gear blank boundaries. The tool cutting edge i will cut the surface S_{i} by its path through the work piece. Two parameters are needed to describe the cut surface, one parameter ξ_{n} along the cutting edge and one parameter ϕ for the position of the tool relative the work piece (in this case the total tool rotation angle). The distance h_0 from the surface S_{i}, cut by the i : th cutting edge, is measured in its surface normal direction $\mathbf{n}_{S_{\mathrm{i}}}$ to the previously cut surfaces. The distance from one point on the surface cut by the i : th cutting edge, to the surface cut by the j : th cutting edge is then given by, see Fig. 3.19.

$$\mathbf{r}_{S_{\mathrm{i}}} - h_0 \frac{\mathbf{n}_{S_{\mathrm{i}}}}{|\mathbf{n}_{S_{\mathrm{i}}}|} = \mathbf{r}_{S_{\mathrm{j}}}\left(\xi_{\mathrm{n}}, \phi\right) \tag{3.10}$$

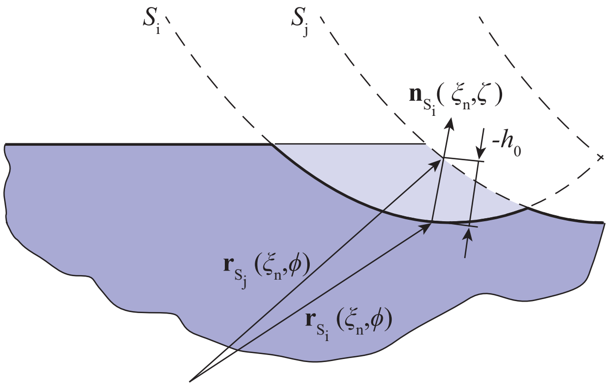

Figure 3.19: Determine the undeformed chip geometry.

Here, the normal direction of the surface S_i is

$$\mathbf{n}_{\mathrm{S_i}} = \begin{pmatrix} n_{\xi,\mathrm{S_i}} \\ n_{\eta,\mathrm{S_i}} \\ n_{\zeta,\mathrm{S_i}} \end{pmatrix} = \frac{\partial \mathbf{r}_{\mathrm{S_i}}}{\partial \xi_\mathrm{n}} \times \frac{\partial \mathbf{r}_{\mathrm{S_i}}}{\partial \phi} = \begin{vmatrix} \hat{\xi} & \hat{\eta} & \hat{\zeta} \\ \dfrac{\partial \xi_{\mathrm{S_i}}}{\partial \xi_\mathrm{n}} & \dfrac{\partial \eta_{\mathrm{S_i}}}{\partial \xi_\mathrm{n}} & \dfrac{\partial \zeta_{\mathrm{S_i}}}{\partial \xi_\mathrm{n}} \\ \dfrac{\partial \xi_{\mathrm{S_i}}}{\partial \phi} & \dfrac{\partial \eta_{\mathrm{S_i}}}{\partial \phi} & \dfrac{\partial \zeta_{\mathrm{S_i}}}{\partial \phi} \end{vmatrix} \tag{3.11}$$

Equation 3.10 can be solved using Newton-Raphson's method. In component form this equation is expressed as

$$\begin{aligned} f_\xi\left(\xi_\mathrm{n}, \phi, h_0\right) &= \xi_{\mathrm{S_j}}\left(\xi_\mathrm{n}, \phi\right) + h_0 \frac{n_{\xi,\mathrm{S_i}}}{|\mathbf{n}_{\mathrm{S_i}}|} - \xi_{\mathrm{S_i}} = 0 \\ f_\eta\left(\xi_\mathrm{n}, \phi, h_0\right) &= \eta_{\mathrm{S_j}}\left(\xi_\mathrm{n}, \phi\right) + h_0 \frac{n_{\eta,\mathrm{S_i}}}{|\mathbf{n}_{\mathrm{S_i}}|} - \eta_{\mathrm{S_i}} = 0 \\ f_\zeta\left(\xi_\mathrm{n}, \phi, h_0\right) &= \zeta_{\mathrm{S_j}}\left(\xi_\mathrm{n}, \phi\right) + h_0 \frac{n_{\zeta,\mathrm{S_i}}}{|\mathbf{n}_{\mathrm{S_i}}|} - \zeta_{\mathrm{S_i}} = 0 \end{aligned} \tag{3.12}$$

Besides the chip thickness $h = h_0 m_\mathrm{n}$, also the position along the cutting edge (ξ_n) and the rotational angle of the tool (ϕ) of the j:th cut surface are unknowns. In matrix format, a solution can be found by

$$\begin{pmatrix} \xi_{\mathrm{n,k+1}} \\ \phi_{\mathrm{k+1}} \\ h_{0,\mathrm{k+1}} \end{pmatrix} = \begin{pmatrix} \xi_{\mathrm{n,k}} \\ \phi_{\mathrm{k}} \\ h_{0,\mathrm{k}} \end{pmatrix} - \mathbf{M}^{-1} \begin{pmatrix} f_\xi\left(\xi_{\mathrm{n,k}}, \phi_\mathrm{k}, h_{0,\mathrm{k}}\right) \\ f_\eta\left(\xi_{\mathrm{n,k}}, \phi_\mathrm{k}, h_{0,\mathrm{k}}\right) \\ f_\zeta\left(\xi_{\mathrm{n,k}}, \phi_\mathrm{k}, h_{0,\mathrm{k}}\right) \end{pmatrix} \tag{3.13}$$

where

$$\mathbf{M} = \begin{pmatrix} \dfrac{\partial f_\xi}{\partial \xi_\mathrm{n}} & \dfrac{\partial f_\xi}{\partial \phi} & \dfrac{\partial f_\xi}{\partial h_0} \\ \dfrac{\partial f_\eta}{\partial \xi_\mathrm{n}} & \dfrac{\partial f_\eta}{\partial \phi} & \dfrac{\partial f_\eta}{\partial h_0} \\ \dfrac{\partial f_\zeta}{\partial \xi_\mathrm{n}} & \dfrac{\partial f_\zeta}{\partial \phi} & \dfrac{\partial f_\zeta}{\partial h_0} \end{pmatrix} = \begin{pmatrix} \dfrac{\partial \xi_{\mathrm{S_j}}}{\partial \xi_\mathrm{n}} & \dfrac{\partial \xi_{\mathrm{S_j}}}{\partial \phi} & \dfrac{n_{\xi,\mathrm{S_i}}}{|\mathbf{n}_{\mathrm{S_i}}|} \\ \dfrac{\partial \eta_{\mathrm{S_j}}}{\partial \xi_\mathrm{n}} & \dfrac{\partial \eta_{\mathrm{S_j}}}{\partial \phi} & \dfrac{n_{\eta,\mathrm{S_i}}}{|\mathbf{n}_{\mathrm{S_i}}|} \\ \dfrac{\partial \zeta_{\mathrm{S_j}}}{\partial \xi_\mathrm{n}} & \dfrac{\partial \zeta_{\mathrm{S_j}}}{\partial \phi} & \dfrac{n_{\zeta,\mathrm{S_i}}}{|\mathbf{n}_{\mathrm{S_i}}|} \end{pmatrix} \tag{3.14}$$

This calculation method will determine the unknown parameters h_0, ξ_n and ϕ using analytically differentiable functions, thus, a convergent solution will especially give the chip thickness $h = h_0 m_\mathrm{n}$ directly without further numerical approximations. This calculation procedure must be repeated to determine the complete chip geometry.

The chip will vary in geometry between the subsequent cuts, due to the machining kinematics, the tool cutting edge geometry, and the gear blank geometry. In gear form milling there are three characteristic chip types, start, full, and exit type chips depending on the tool position relative the gear blank, see paper VI. In gear hobbing substantially more chip types are cut by the many active hob cutting teeth. The chips cut by both the form milling cutter and the hob have a complex shape, and vary heavily in width, length, and thickness, see paper VI, paper VII, or reference [10].

In industrial conditions errors related to the tool or the machine are most often present, such as axial and radial positional errors to the cutting teeth, eccentricity, etc.. These possible errors will give further variations of the chip geometry, also between subsequent cuts. The effect of tool run-out and eccentricity errors are analyzed in the study performed in paper VI.

3.3.2 Cutting Forces

With a detailed description of the chip geometry established, it is possible to predict the cutting forces. Most machining operations, where a chip is sheared off by a cutting tool, are governed by the same mechanism. The chip deformation is essentially plane strain [36], since the chip width is very large compared to the undeformed chip thickness. This approximation is used in several methods where the cutting forces are predicted, examples are the finite element method [37, 38], the slip-line field theory [39, 40], and the mechanistic approach [41].

The cutting forces acting on the tool can directly be predicted using slip-line field theory or by the finite element method. Slip-line field theory applies to plane strain plastic flows [42], where the deformation occurs under

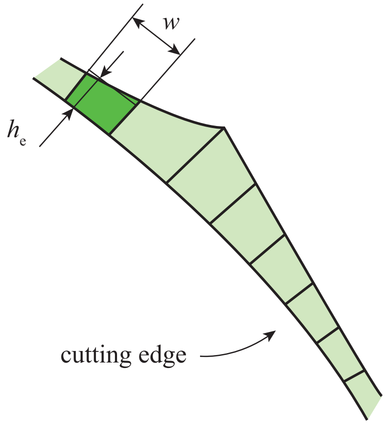

Figure 3.20: Portion of a chip that is discretized into elements.

steady state conditions. Commercial finite element packages can predict the cutting forces in three dimensions, however, these are very computational time consuming. A majority of the presented research is limited to two-dimensional analysis, see e.g. [37, 38, 43], and still requires great computational effort. The more geometrical complex chip geometry and the great variety of chip forms in gear milling would make it practically impossible to calculate the instantaneous cutting forces using the finite element method. At least if the full production cycle should be considered. In case of both slip-line models and finite element models several unknown parameters need to be established in order to derive an accurate force prediction model. Therefore, the mechanistic approach is used to determine the tool cutting forces in this work. Here, the cutting force parameters are experimentally established by an equivalent machining process. The fast cutting force calculation procedure makes it possible to consider the complete gear milling operation, from the first to the last cut, and the cutting forces are predicted with sufficient degree of accuracy, see paper VI.

The instantaneous chip cross section is divided in elements along the cutting edge, see Fig. 3.20. Incremental cutting forces act on each element, where each element has the chip width w and the mean chip thickness h_{e}. It is well known from metal cutting theory, that the cutting forces increase proportional to the undeformed chip thickness. The proportionality factor depends on the tool/work piece interaction, the material being cut, the cutting speed, etc.. Different proportionality factors are presented in literature, for example, linear [41], polynomial [44] and power-law (Kienzle)[45], where all of these are based on curve-fitted functions based on

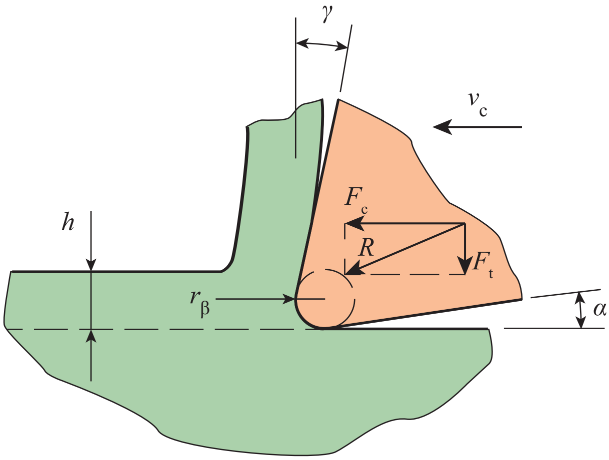

Figure 3.21: Plane view of chip removal perpendicular to the cutting edge. The cutting speed v_{c}, instantaneous chip thickness h, cutting edge radius r_β, rake angle γ and clearance angle α.

experimental data.

Each element is considered as two dimensional, see Fig. 3.21, and with no interaction with its neighbor. In this work, a linear force model is used to determine the instantaneous cutting forces for each element along the cutting edge. The incremental cutting force are

$$\begin{aligned} dF_{\mathrm{c}} &= \left(K_{\mathrm{c,c}} h_{\mathrm{e}} + K_{\mathrm{c,e}}\right) w \\ dF_{\mathrm{t}} &= \left(K_{\mathrm{t,c}} h_{\mathrm{e}} + K_{\mathrm{t,e}}\right) w \end{aligned} \tag{3.15}$$

Here, $K_{\mathrm{c,c}}$, $K_{\mathrm{t,c}}$ are the cutting force coefficients and $K_{\mathrm{c,e}}$, $K_{\mathrm{t,e}}$ are the edge force coefficients [41]. With the approximation that no force interaction take place between the discretized elements, the total instantaneous cutting force equals the sum of all elements along the edge line.

This methodology is applied in paper VI to determine the cutting forces in gear form milling, and in paper VII to determine the cutting forces in gear hobbing, where the implementation to each of these manufacturing processes are described.

3.3.3 Verification of Cutting Forces

In gear milling it is difficult to validate the cutting forces acting on the tool itself, limited space, telemetry data acquisition, rotating tool and work piece are reasons to name a few. The cutting forces are measured using a

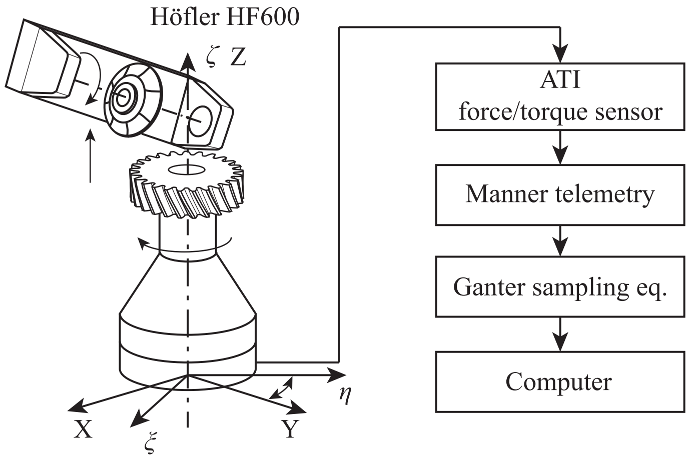

Figure 3.22: Experimental set-up in cutting force measurement.

measurement system developed at Sandvik Coromant. The experimental set-up is displayed in Fig. 3.22, where the gear blank is directly screwed to a force/torque sensor which in turn is attached to the hob machine's rotary feed table. A Ganter sampling equipment is sampling the raw data at 2500 Hz by a Manner telemetry system. The data is thereafter post processed in a computer, by such as filtering techniques.

As the cutting forces are measured on the gear blank, the rotation of the rotary feed table must be taken into account. Using a form milling cutter, the rotary feed table is stationary when spur gears are cut, and rotating when cutting helical gears. The feed table is indexed to the next position to cut the next tooth space. The cutting forces are measured in the X, Y, and Z directions of the sensor's reference system, so to be able to compare the cutting forces of each tooth gap, the measured forces must be transformed to a reference position. The predicted cutting forces in gear form milling are verified by use of this experimental set-up, see paper VI.

3.3.4 Tool Wear

Tool life has a strong economic impact in machining operations [46], thus it is important to development quantitative models for prediction of tool life. Tools degrade by damages during operation. The tool cutting edge can degrade by a continuous loss of material, or by sudden loss of material due to accumulation of cracks that lead to fracture. Tool degradation by continuous material loss is classified as wear [28]. The wear rate depends on many factors, such as thermal and mechanical loads, work piece material, lubrication etc., and the tool deteriorate rapidly by plastic deformation, chemical reaction, and chemical diffusion [42]. Tool wear is often classified as [28]

- Abrasive wear
- Adhesive wear
- Diffusion wear
- Chemical and electro-chemical wear

In the field of metal cutting, different tool life prediction models are presented in research. In turning, especially, Taylor tool life equation [47] is widely used

$$v_\mathrm{c}\, T^\mathrm{n} = C \tag{3.16}$$

The Taylor life curve gives the relation between cutting speed v_c and expected tool life T, where n and C are constants. The modified Taylor tool life equation, to account for the feed f and the depth of cut d [42], is

$$v_\mathrm{c}^{(1/\mathrm{n_1})}\, f^{(1/\mathrm{n_2})}\, d^{(1/\mathrm{n_3})} T = C' \tag{3.17}$$

or alternatively [46],

$$v_\mathrm{c}\, f^{(1/\mathrm{n_1})}\, d^{(1/\mathrm{n_2})}\, T^{(1/\mathrm{n_3})} = C' \tag{3.18}$$

where n_1, n_2, n_3, and C' are constants. Additionally, Colding presented three tool life equations to predict the expected tool life [48, 49, 50]. Both Taylor's and Colding's equations are curve fitted functions based on experimental data, where the tool's end-of-life criterion must be reached. This requires that a great number of costly experiments must be performed in order to determine the tool life equation constants. And this have to be done for each tool and work piece combination, and in case of Eq. 3.16 for each feed rate and depth of cut. Moreover, these models are only useful where the load position along the cutting edge is stationary, like in turning for example. In gear milling, in contrast, the load along the cutting edge varies heavily due to the chip thickness variation, and each position along the cutting edge cuts varying accumulated chip length.

Figure 3.23 shows the typical wear behavior of a hob cutting tooth. Crater wear is present on the rake face and flank wear on the clearance face. On the corner of the hob cutting tooth, increased flank wear is common, called hollow

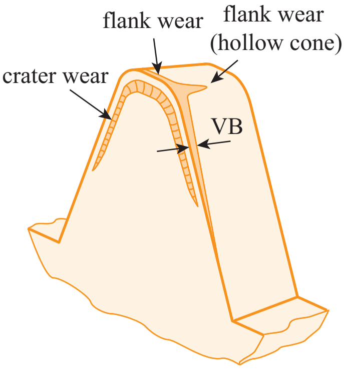

Figure 3.23: Typical wear of cutting teeth [29].

cone flank wear. Hoffmeister studied the wear on hob teeth at one position of each hob cutting tooth. According to Hoffmeister [29], the progression of the flank wear and the crater wear mainly depends on the accumulated chip length, whereas the distance from the cutting edge to the crater wear depends on the chip thickness. To further study the hob's wear behavior, a wear model that incorporate both the cutting edge load and the cut chip length is needed.

Abrasive wear is dominant in gear milling. An abrasive wear prediction model that incorporates tool load and cut chip length is the Archard's wear model [51, 52], or by Usui's wear model, which is a modified version of Archard's, that account for cutting temperature [53]. Archard's original wear model [54] is a physical wear model that reads

$$V = K\,N\,s \tag{3.19}$$

where the volumetric loss V is proportional, K, to the normal surface force N and the sliding distance s, i.e. chip length. The constant K depends on the material hardness. In paper VI the worn volume is expressed by the flank wear VB

$$V = \frac{1}{2}\,\mathrm{VB}^2\,\frac{\tan\gamma_{\mathrm{min}}}{1-\tan\gamma_{\mathrm{min}}\tan\gamma_{\mathrm{maj}}}\,w \tag{3.20}$$

Combining Eq. 3.19 and Eq. 3.20, and dividing with the contact area $A = \mathrm{VB}\,w$, the flank wear progression can be expressed as

$$\mathrm{VB} = 2\,K\,p\,s\,\frac{1-\tan\gamma_{\mathrm{min}}\tan\gamma_{\mathrm{maj}}}{\tan\gamma_{\mathrm{min}}} \tag{3.21}$$

In order to determine the flank wear, the pressure on the clearance face is needed. In paper VII the simplification is used that the pressure level is

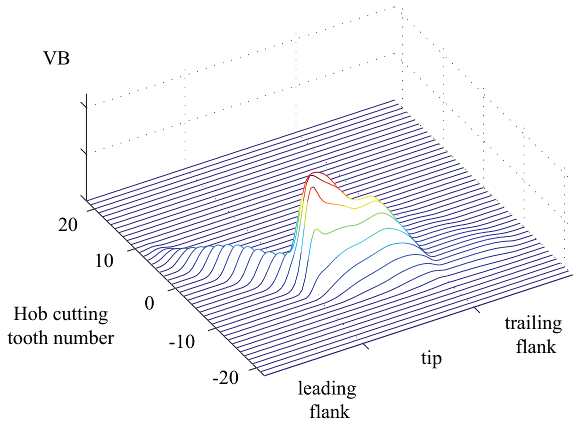

Figure 3.24: Wear behavior along the cutting edge of all the hob's cutting teeth, from paper VII.

constant on the rake and the clearance face. The pressure on either side of the cutting edge must be in equilibrium with the instantaneous cutting forces.

The constant K in Archard's wear equation is at this stage unknown, so a quantified determination of the wear is not possible. However, the wear behavior of the individual hob cutting teeth at any position along the edge line can be predicted. This is presented in Fig. 3.24, which is one of the results from paper VII. To be able to predict the wear behavior in this way would be valuable input to in advance make a predictive decisions on shift strategies, where shift strategies used in industry today are decided based on empiricism [4]. The tools end-of-life is not possible to predict without a quantified determination of the wear.

Chapter 4

Summary of Appended Publications

Seven papers are appended to this thesis. A summary of each paper is given below.

Paper I: Tooth Deviation of an Involute Helical Gear Manufactured in a Simulated Hobbing Process with Introduced Errors

Gear hobbing is a geometrically complex machining process, where several integral parameters affect the produced gear tooth quality. Close to ideal values of the machine parameters are hard to achieve in practice, and tool geometrical errors are most often present. By these possible errors the designer accepts small deviations on the gear tooth given by the manufacturing tolerances. The manufacturer's task is to effectively and economically meet these tolerances.

It is, however, hard to link possible machine and tool related errors to the machined gear tooth deviations, but this link is needed to be able to improve the manufacturing process. Therefore, a mathematical model is developed to calculate the machined gear tooth surface topography, where error sources common in industrial applications are considered. The error sources introduced in the model can be either isolated error sources or combined error sources, in order to see how the machined gear tooth surface is affected. The errors considered in the model are linked to the machine settings by, center distance, cross angle, tilted gear axis (or oblique tool sled), and eccentricity to the tool axis, compared to the ideal setting. Multiple start hobs are frequently used in industry to increase productivity.

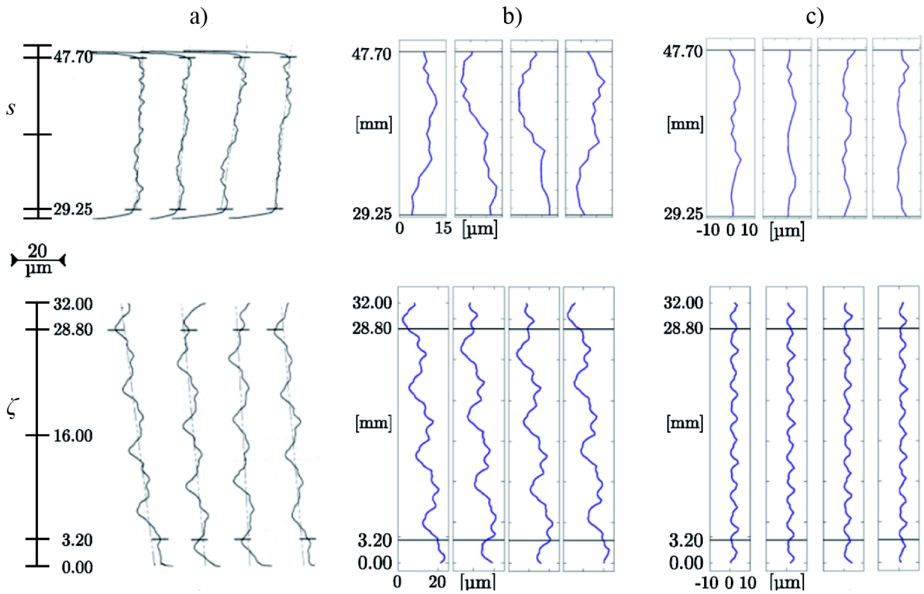

Figure 4.1: Graphical inspection charts. a) Experimental result, b) simulated result under reference conditions, c) Simulated under ideal theoretical conditions.

These hobs are, however, prone to geometrical deviations between hob threads compared to one start hobs. Positional errors of hob teeth were therefore also included in the mathematical model as tool related errors.

The mathematical model was validated by an experimental study. Gear wheels were cut in an industrial hobbing machine, where deviations were intentionally introduced to the machine settings and the process parameters. The same deviations were introduced in the mathematical model. The cut and the calculated gear teeth are compared by inspection charts in Fig. 4.1, and good agreement is achieved. This measurement procedure is explained in Ch. 3.2.2.

In this study, additional errors to the manufacturing process were identified, where these errors were a tilted gear axis and positional error to one of the three hob threads. The tilted gear axis can, however, be compensated for in the machine setting by changing the center distance as the hob travels over the gear width.

Paper II: The influence of Tool Tolerances on the Gear Quality of a Gear Manufactured by an Indexable Insert Hob

The eternal strive in industry is to increase productivity. New type of gear cutting tools, with indexable carbide inserts, are introduced on the market which are capable of working at significantly higher feed rates and cutting speeds compared to high speed steel hobs. The hob with inserts, where each individual insert is fixed on a tool body is, however, prone to positional errors of the cutting edges. A lot of empiricism exist in industry on the expected gear tooth quality cut by HSS hobs, but, little experience exist for the new indexable insert hobs. The motivation of this paper is therefore to focus on the achievable gear tooth quality cut by different hob quality classes, where the positional errors to the cutting teeth are typical for indexable insert hobs.

This study use a Monte Carlo approach to calculate the gear tooth surface topography machined by different hob quality grades. The magnitude of the cutting teeth's positional errors are according to DIN 3968 classification of the hob quality classes AA, A, B, and C, where the positional error distribution are assumed to comply with a Gaussian distribution. In the mathematical model, hobs are generated within these hob quality classes, which virtually cut gears to determine the gear tooth surface topography. Based on the gear tooth deviations described in Ch. 3.2.2, the gear quality is graded according to DIN 3962 Part 1 and 2. This work flow is illustrated in Fig. 4.2. The result from this study gives the expected gear tooth quality cut by different hob quality classes at different feed rates, see Fig. 4.3.

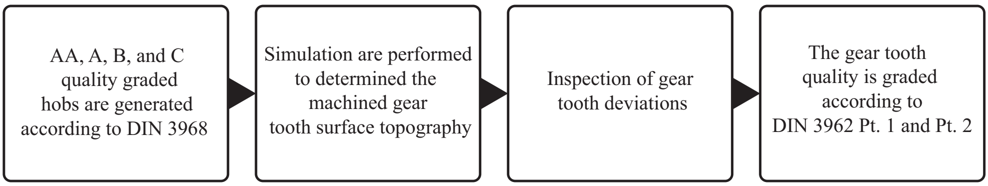

Figure 4.2: The work flow used in this study in order to assess the gear tooth quality machined by different hob quality classes.

The model is validated by experimental results. A physical hob with indexable inserts is inspected, and the measured positional errors of each hob cutting tooth is used as input to the mathematical model. The physical hob cuts a gear wheel, which is inspected for tooth deviations. The inspection charts of the cut gear are compared with calculated results, which shows good agreement.

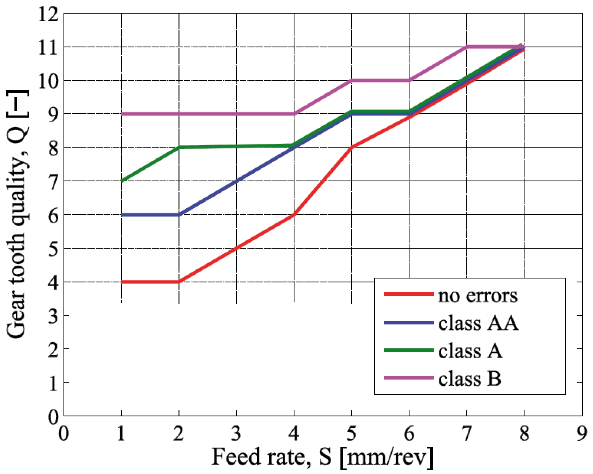

Figure 4.3: Gear tooth quality vs. axial feed rate of hob for different hob classes. The most accurate gear tooth is given by the lowest gear quality number.

The gear tooth surface is most often refined after the roughening cut in a subsequent operation. Refinement is especially needed for gears that are machined by lower quality hobs and at increased feed rates. To be able to refine the gear teeth a machining allowance is needed. The gear teeth are cut using a protuberance tool to acquire grinding stock. The grinding stock should be sufficient to swallow imperfections from the milling operation, but minimizing it would definitely promote the subsequent refining steps. The required amount of grinding stock cannot be controlled by the gear inspection charts, as only relative errors are determined. In the model, however, the cut gear tooth surface is compared to the ideal gear tooth geometry, which offers the possibility to determine the minimum amount of grinding stock needed. The minimum amount of grinding stock is presented in this paper for different feed rates and hob quality classes.

Paper III: Prediction of alignment deviations on a lead crowned helical gear manufactured by a hob

A common problem in gear transmissions is to achieve alignment of the gear axes. In general perfect alignment is hard to achieve, and with changing transmitted torque the gear wheels will tilt due to beam deflection. Cylindrical gears on parallel axes will have line contact if perfectly aligned, and point contact if they are not. If point contact is present by non-aligned

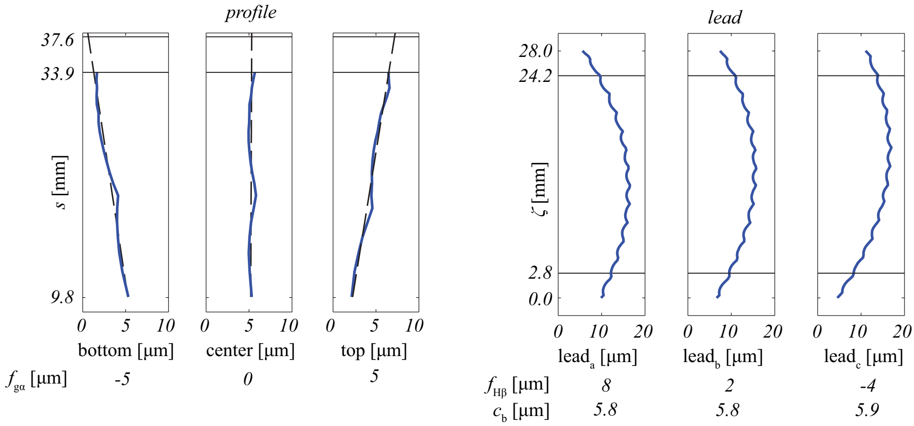

Figure 4.4: Calculated graphical inspection charts. Cross and square measurements are combined in order to capture flank twist.

axes, the contact will be at tooth ends where the gear teeth are most vulnerable. To avoid hard bearing at tooth ends, lead crown modification is added to center the load.

Lead crown modification can be manufactured using a hob, and is achieved by varying the center distance while the hob is fed along the face width of the gear. This method is used in both hob milling and hob grinding operations. One drawback when using this method is that alignment deviations always will arise on helical gear tooth profiles. Figure 4.4 shows calculated inspection charts where cross and square measurements are combined to capture flank twist. Flank twist is well known in literature, but no model has previously been able to give quantitative predictions of the alignment errors.

The allowed manufacturing tolerances are specified on the drawing provided by the designer, where gear tooth alignment deviations are included. It would therefore be of greatest interest to in advance be able to predict these alignment deviations. It would then be possible to determine if the gear could be manufactured within tolerances by this manufacturing method. This paper explains the reason why alignment deviations arise when hobbing lead crowned gears. The analysis shows that these deviations always will occur when using a hob, and the least expected profile alignment deviation is

$$f_{g\alpha} = 4C\frac{\Delta s_{\mathrm{p}}}{\Delta b}\tan\beta_{\mathrm{b}} \tag{4.1}$$

and the lead alignment deviation is

$$f_{\mathrm{H}\beta} = 4Cb\frac{\Delta s_{\mathrm{l}}}{\Delta b^2}\tan\beta_{\mathrm{b}} \tag{4.2}$$

To obtain stable results, a practical guideline for the feed rate is

$$S \leq \frac{\Delta s_{\mathrm{p}}\tan\beta_{\mathrm{b}}}{2} \tag{4.3}$$

If the alignment errors predicted by Eq. 4.1 and Eq. 4.2 exceeds the pre-specified tolerances, another manufacturing method should be used that does not have this inherent error.

Paper IV: Gear Tooth Surface Roughness of Helical Gears Manufactured by a Form Milling Cutter

Gear form milling cutters have long been out rivaled by more efficient tools, such as hobs. However, the form milling cutter is competitive in special cases. Cheap tooling makes the milling cutter suitable to small series production and prototypes. Total production time can be competitive using multitasking machines, where gear integrated components can be machined complete in one set-up. Moreover, indexable insert milling cutters have been introduced on the market that are capable to substantially increase productivity.

The main disadvantage of form milling cutters is that the cutter cannot cut a wide range of gear teeth, it is not universal. Instead, the form milling cutter must be purpose designed for the gear geometry to cut. In this paper, the geometry of the milling cutter is derived, in parametric form using inverse calculation, so that a cutter can machine spur or helical gears correctly.

The paper presents a mathematical model that is able to calculate the machined gear tooth surface topography. The model is validated by experiments, where a gear is cut using an indexable insert form milling cutter. The radial position of the milling cutter's teeth were measured prior to machining, where the measurements showed that these deviations were significant. Thus, positional errors to the cutting edges and eccentricity of the tool rotational axis were introduced into the model. The measured positional errors were used as input to the mathematical model.

Inspection charts measure the gear tooth along designated lines, but a lot of information is lost by few line measurements alone. In this study a surface area measurement is performed of the machined gear tooth using a computer numerically controlled optical microscope, *Alicona Infinite Focus*. Figure 4.5 compares the calculated and measured tooth surface, and the agreement is remarkable.

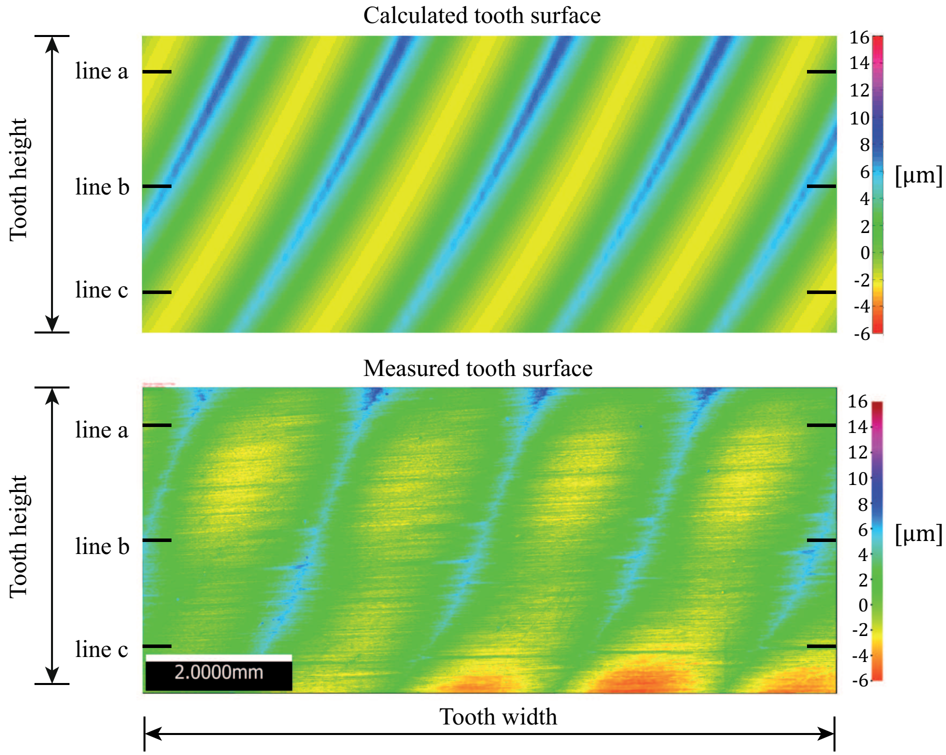

Figure 4.5: Comparison between the calculated and the measured tooth surface topography machined by a form milling cutter.

Paper V: The Undercut Criterion of Pinion Shaper Cutters - and an Improvement by Modifying the Basic Rack Profile

The gear tooth geometry is normally defined by its conjugate basic rack. The basic rack defines the complete gear tooth geometry, including the fillet. The gear fillet can, however, be undercut if the designer does not take care. This type of undercut is well known, and is undesired as it may weaken the gear tooth. This type of undercut is avoided if

$$z \geq 2\cos\beta \frac{h_{0,\mathrm{t}} - x - r_{0,\mathrm{t}}\,(1 - \sin\alpha_{\mathrm{n}})}{\sin^2\alpha_{\mathrm{t}}} \tag{4.4}$$

and it is the designer's responsibility that this type of undercut does not happen.

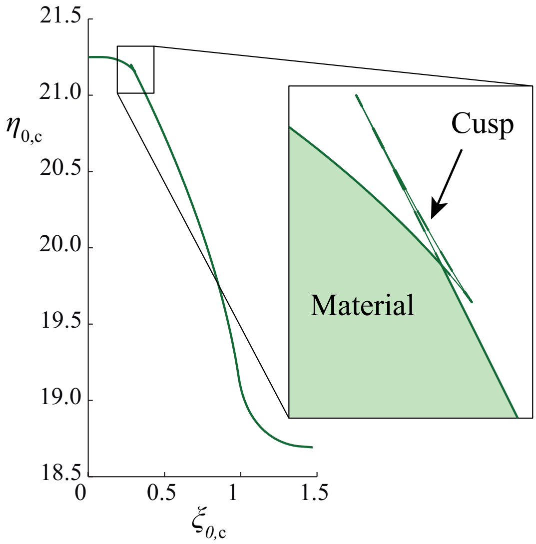

Figure 4.6: Undercut tip of shaper cutter tooth.

It is the manufacturer's task to produce the designed gear regardless of manufacturing method chosen. To cut the designed gear tooth, the manufacturer should choose a tool conjugated to the same basic rack. In some cases, the pinion shaper cutter is the only appropriate tool, for example, if the gear tooth is adjacent to a shoulder. However, if the gear is conjugated to the standard basic rack with a circular fillet, it is in this paper derived that very large tooth numbers are needed to not undercut the tip of the tool, see Fig. 4.6. An undercut tool tip will not produce the correct gear fillet. The minimum tooth number needed to avoid an undercut tool tip is

$$z \geq z_{\min} = 2h_0(\alpha_{\mathrm{n}})\frac{\cos\beta}{\sin^2\alpha_{\mathrm{t}}}\left(\frac{h_0(\alpha_{\mathrm{n}})}{r_{0,\mathrm{t}}\cos\alpha_{\mathrm{n}}}\frac{\cos\beta}{\tan\alpha_{\mathrm{t}}}\frac{\tan^2\alpha_{\mathrm{n}}+1}{\tan^2\alpha_{\mathrm{n}}+\cos^2\beta}-1\right) \tag{4.5}$$

It is shown that, the standard shaper cutter with a circular tip rounding is, at least very closely, conjugate to a rack with an elliptical fillet. This cutter will, however, cut a fillet geometry different from the fillet defined by a basic rack with a circular fillet. The fillet geometry is rarely control measured after the gear is cut, but it should certainly be manufactured according to the specifications. If the shaper cutter is the only appropriate tool, a revision should be made if an elliptical fillet is sufficient. With an elliptical fillet to the basic rack, a new undercut criterion was derived

$$z \geq z_{\min} = 2h_0(\alpha_\mathrm{n})\frac{\cos\beta}{\sin^2\alpha_\mathrm{t}}\left(\frac{h_0(\alpha_\mathrm{n})}{\tan\alpha_\mathrm{t}}\frac{d\varphi_\mathrm{t}}{d\varphi_\mathrm{n}}\frac{1}{\frac{dh_0}{d\theta}}\frac{1}{\frac{d\theta}{d\varphi_\mathrm{n}}} - 1\right) \tag{4.6}$$

Without interfering on the involute profile on the cut gear, the shaper cutter could have a lot fewer teeth without undercutting the tooth tip. To not, unintentionally, undercut the fillet of the gear to cut, Eq. 4.4 must be modified accordingly

$$z \geq 2\cos\beta\frac{h_{0,\mathrm{t}} - x - r_{0,\mathrm{t},\eta}\left(1-\cos\theta\right)}{\sin^2\alpha_\mathrm{t}} \tag{4.7}$$

Paper VI: Prediction and Experimental Verification of the Cutting Forces in Gear Form Milling

A mathematical model is presented that predicts the cutting forces in gear form milling. To be able to predict the cutting forces a detailed determination of the chip geometry is first needed. The chip geometry is determined by comparing the paths of the milling cutter's cutting edges. The volumetric difference by the successive cuts equals the undeformed chip geometry. Thus, to determine the chip geometry, the cutting edge geometry and its cutting path must be known. The cutting edge geometry of the milling cutter is derived in parametric form as described in paper IV. The chip geometry is directly solved by an analytical differential description in order to minimize numerical errors.

The cutting forces are resolved using the mechanistic approach. By using this approach, the chip geometry is discretized into elements, where each element is regarded as two dimensional. On each element incremental cutting forces act, which are experimentally determined and in this case proportional to the instantaneous undeformed chip thickness. The total load on the tool is determined by summing the contribution of each element along the complete edge length.

In order to validate the mathematical model, gear tooth gaps were cut using two different indexable insert form milling cutters, $\mathrm{m_n} = 5\,\mathrm{mm}$ and $\mathrm{m_n} = 7\,\mathrm{mm}$. The milling cutters used in the experimental study had run-out and eccentricity errors. These errors were introduced in the model, as in paper IV. These errors are important to consider, as they will lead to variation in cut chip geometry and consequently in variation of the cutting forces.

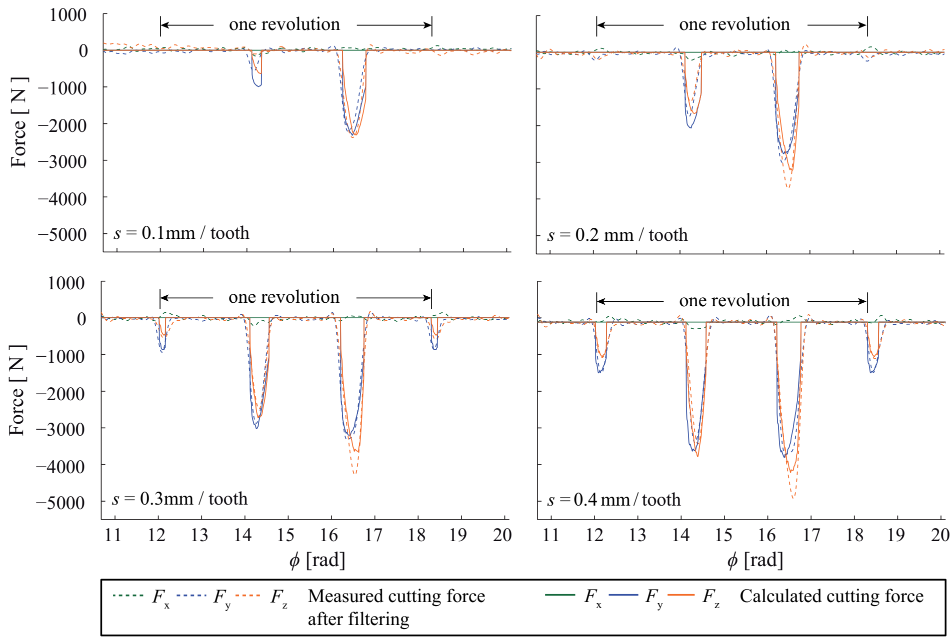

Figure 4.7: Cutting forces in X,Y,Z-direction of the module 5 cutter with 3 active cutting teeth. This plot display the influence of positional errors and eccentricity to the tool at the four feed rates s = 0.10 , 0.20 , 0.30 , and 0.40 mm / tooth.

Gear tooth gaps were cut in an industrial hobbing machine, and the cutting forces were measured on the work piece, see experimental set-up in Ch 3.3.3. The two milling cutters were tested at the feed rates s = 0.10, 0.20, 0.30, and 0.40 mm / tooth. The shape of the calculated and measured force curves agree well, and the peak force levels were predicted within 12 % when considering both cutters and the complete feed series.

Figure 4.7 shows the predicted and the measured cutting forces at the four feed rates studied using a $m_n = 5$ mm cutter with three active cutting teeth. The cutting force variation is due to the run-out and eccentricity errors. The cutting forces were successfully predicted for different size cutters and feed rates.

Paper VII: Prediction of the cutting forces in gear hobbing and the wear behavior of the individual hob cutting teeth

Tool life has a strong economic impact in gear hobbing, where the tool life is normally limited by the tool wear that progress during the milling operation. Shift strategies are used in industry to try to achieve an even wear distribution of the hob's cutting teeth. These strategies are today based on empiricism, but, to make predictive decisions in order to make the tool wear even and consequently optimize tool life, the tool wear must be determined.

In order to predict the wear of the complete hob, the load along the cutting edge of all the hob's cutting teeth must be known. Thus, a detailed description of the chip geometry and the cutting forces are needed. In this paper, a mathematical model is presented that calculates the cutting forces in hob milling using the mechanistic approach, where the undeformed chip geometry is continuously determined by an analytical differential description presented in previous research [10]. The fast calculation method makes it possible to consider the full production cycle, from the first to the last cut. Figure 4.8 shows the cutting forces acting on the hob during the complete machining

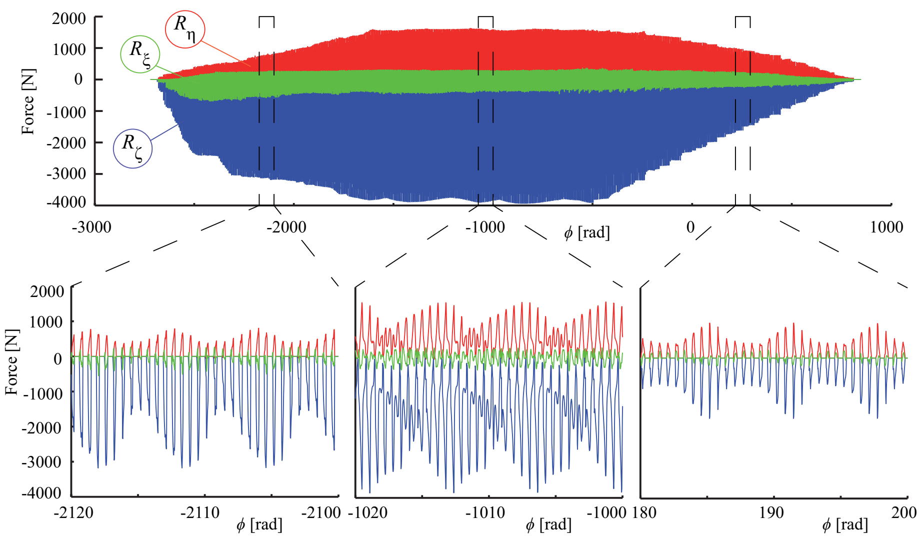

Figure 4.8: Calculated cutting force of the hob at feed rate $S = 2.0\,\mathrm{mm}\,/\,\mathrm{rev}$. The top diagram display the cutting forces of the complete production cycle. The bottom enlarged diagrams display the three characteristic regions, entry, full, and exit.

of a gear wheel. Considering the full production cycle is not considered in previous research, but is needed to predict the accumulated wear and the wear behavior of each individual hob cutting tooth.

The normal situation when choosing process data in gear hobbing is to limit the maximum chip thickness, which consequently limits the cutting forces and the load on the hob's cutting teeth. Hoffmeister's formula is used in industry to predict the maximum chip thickness, however, this formula is based on an approximate hob chip model. A comparison is made between the chip thickness calculated by this model and Hoffmeister's formula, which shows that Hoffmeister underestimates the maximum chip thickness, at least in the numerical example presented.

The tool wear is predicted using Archard's wear model, which incorporates the tool load and the cut chip length (i.e. sliding distance). The wear constant in Archard's wear model is unknown at this stage, so a quantitative prediction of the tool's end-of-life is not possible. However, it is possible to predict the wear behavior of all cutting teeth, see Fig. 3.24. To be able to predict the wear along the complete cutting edge length of each individual hob cutting teeth is valuable input when selecting shift strategies.

Chapter 5

Conclusions and Future Work

5.1 Conclusions

Gear wheels are a fundamental part within several industrial and engineering applications. The modern requirements on power transmissions focus on energy efficiency, low noise and dynamic vibration, and high power density. This demands that the gear wheels are manufactured to very high precision. It is also required that these gear wheels are manufactured with economical awareness. To be able to improve gear manufacturing, for example by increasing efficiency, accuracy and productivity, deep knowledge and understanding of the manufacturing processes are needed. In this thesis, several topics concerning manufacturing of cylindrical helical gears are analyzed. Mathematical models have been developed to be able to resolve the posted research questions. These models have been validated in experimental studies performed in industrial conditions.

The first research question (R. Q. 1) is on prediction of the machined gear tooth surface topography. If the gear is finished cut, the machined tooth surface has a significant impact on how the gears will perform in operation. If the gear tooth surface will be resurfaced after the milling operation, it is desired to have a controlled tooth surface topography in order to make the time consuming and costly refining steps easier. Additionally, the fillet region is most often unchanged after the refining steps, and in this highly stresses region, a controlled surface topology is needed to keep the stresses sufficiently low. All of these aspects are connected to the process parameters, and possible tool and machine related errors. It is therefore of great importance to in advance be able to predict the machined tooth surface in process planning, considering process parameters, and possible tool and machine related errors.

This work shows that it is possible to calculate the expected gear tooth surface using the presented mathematical models where these considerations are taken into account. The tool and the process related errors that are incorporated into the models are common in industrial conditions. Experimental studies are performed in order to validate the mathematical models, see paper I, II, and III for gear hobbing and paper IV for gear form milling. The agreement is good, which shows the industrial applicability of the models in milling operation.

The mathematical models that predict the machined gear tooth surface have shown industrial applicability in hob grinding operations as well, not only in hob milling operations. In paper III, the model has been able to support the analytical analysis of flank twist, which is also experimentally verified. This paper also presents analytic equations that predicts the magnitude of the alignment errors that will arise when lead crowning helical gear using a hob. These equations are already in industrial use.

Further, in order to manufacture the intended gear geometry, it is important that the tool geometry is correct. The gear geometry is in this work defined by its basic rack design, and under this premise, the tool must share a mutual basic rack to cut this gear correctly. There is, however, a risk that the tip of the tool can be undercut. If the tool is undercut in this way, it will not produce the correct gear fillet. The criterion that must be met to avoid this type of undercut is derived in paper V. This paper use the shaper cutter as an example, but the undercut criterion is applicable to all tools conjugate to the basic rack, such as hobs and skiving cutter. The undercut criterion is critical for smaller helical angles, relevant for shaper and skiving cutters, and it is shown that very large tooth numbers are needed if the tool is conjugate to the basic rack with a circular fillet. However, a significant reduction of the minimum tooth number is suggested by a modification to the basic rack profile.

The second research question (R. Q. 2) is on prediction of the tool cutting forces and tool wear. The tool wear is usually the criterion for the tool's end of the service life. Tool life has a strong economic impact in machining operations, thus, development of quantitative models for prediction of tool life is an important part in any machining process. To predict tool wear, a detailed description of the chip geometry and the tool cutting forces are needed. It was not possible with the existing measurement techniques to measure the cutting forces acting on each individual cutting tooth in the hob milling operation. If the total force is measure on the hob it is hard to separate the cutting force acting on each cutting tooth, as several cutting teeth are removing material simultaneously and the chip geometry varies heavily between the subsequent cuts. Thus, it would be very hard to validate the results from the mathematical models. Instead a diversion was made to study the less complex form milling operation.

Gear form milling was experimentally studied using single and multiple tooth cutters. Multiple tooth cutters were studied in order to account for tool eccentricity and run-out errors, as these errors are common in industrial applications, and lead to chip geometry and cutting force variations. A mathematical model was developed to calculate the cut chip geometry in gear form milling, where these tool errors are considered. With a detailed description of the chip geometries cut by the form milling cutter, the cutting forces were predicted using the mechanistic approach. The cutting forces were experimentally verified by the experimental set-up described in Ch 3.3.3. The mathematical model showed good agreement between calculated and measured results, where both the force levels as well as the shape of the force curve during the complete immersion angle were successfully predicted for different size cutters and varying feed rates. This was also the case when tool related errors were considered. The knowledge gained from gear form milling was thereafter applied to gear hobbing.

The hob model is able to calculate the total cutting force acting on the complete hob as well as calculating the isolated cutting forces acting on each individual hob cutting tooth. The fast calculation scheme makes it possible to in detail calculate the geometry of all cut chips and the cutting forces acting on each cutting edge for the complete production cycle. To consider the full production cycle is needed to predict the accumulated load on the tool, which is important to be able to estimate the wear progression on the tool completely.

The tool wear was predicted using Archard's wear model. A quantitative determination of the wear was not possible since Archard's wear constant is unknown at this stage, however, the wear behavior of the tool was predicted along the complete cutting edge length of each individual hob cutting tooth. To predict the wear behavior in this way is valuable input when determining shift strategies, which are used to try to achieve close to even wear of all hob cutting teeth.

It is in this work shown that it is possible to calculate the chip geometry and the cutting forces in gear hobbing and gear form milling, and to predict the wear behavior of the hob's cutting teeth using the presented mathematical models.

5.2 Future Work

The work presented in this thesis is a step forward in a better understanding of the complex machining processes involved in gear manufacturing. The mathematical models that are developed have been able to answer several questions and support the analyses performed in this thesis. During the progression of this work several more, yet unanswered, questions have arisen. This section discuss two topics that should be investigated further.

Tool wear prediction is one topic that need further study, which has already been pointed out in Ch. 3.3.4. Is was not possible to give a quantitative prediction of tool wear without Archard's wear constant K. This constant is at this stage unknown, and must be experimentally determined and verified in order to predict the tool wear. It would be possible to give quantitative predictions of the tool wear if this constant is known. This is needed in order to give predictive decisions, to optimize tool utilization, prolong tool life, and to predict the tool's end-of-life.

In paper VII a comparison was made of the maximum chip thickness $h_{\max}$ determined by Hoffmeister's formula and the chip model used in this thesis. Hoffmeister's formula is a curve fitted function based on an approximate hob chip model. This formula is currently widely used in industrial process planning by its simple way to estimate the maximum chip thickness, where it is desired that the maximum chip thickness should not be too large. The comparison made in paper VII shows, however, that Hoffmeister underestimates the maximum chip thickness. The industrial empiricism is based on the chip thickness predicted by Hoffmeister's formula, but there is an opportunity to develop a more exact formula based on the hob chip model presented by Vedmar [10].

Bibliography

[1] Dudley D. W., 1969 *The Evolution of the Gear Art,* American Gear Manufacturers Association, Washington D.C., USA.

[2] DIN 867, 1986, Basic Rack Tooth Profiles for Involute Teeth of Cylindrical Gear for General Engineering and Heavy Engineering.

[3] Vedmar L., Henriksson B., 1998, A General Approach for Determining Dynamic Forces in Spur Gears, AMSE Journal of Mechanical Design, 120, 593-598.

[4] Endoy R., 1990, *Gear Hobbing, Shaping and Shaving - A Guide to Cycle Time Estimation and Process Planning*, Society of Manufacturing Engineers, Dearborn, Michigan, USA.

[5] SMS 1861, 1972 Cylindrical Gears - Basic Rack with Tip Relief, 2. ed, SMS - Sveriges Mekanstandardisering, Stockholm, Sweden.

[6] SMS 3037, 1977 Cylindrical Gears - Basic Rack with Tip Chamfer and Machining Allowance for Shaving, 1. ed. SMS - Sveriges Mekanstandardisering, Stockholm, Sweden.

[7] Vedmar L., 2010, A Parametric Analysis of the Gear Surface Roughness After Hobbing, ASME Journal of Mechanical Design, 131:111004–1 – 111004–8.

[8] Sjöberg S., 2014 Influence of Running-in on Gear Efficiency, KTH Royal Institute of Technology, Doctoral Thesis, ISBN 978-91-7595-258-1, Stockholm, Sweden.

[9] Merritt, H. E., 1962, *Gears*, 3rd ed., Sir Isaac Pitman & Sons, London, UK.

[10] Vedmar L., Andersson C., and Ståhl J-E, 2009, A Parametric Analysis of the Undeformed Chip Geometry in Gear Hobbing. ASME Journal of Manufacturing Science and Engineering, 131:061003–1 – 061003–8.

[11] Goch G., 2003, Gear Metrology, CIRP Annals - Manufacturing Technology, Vol. 52, Issue 2, 659-695

[12] VDI/VDE 2606, 2010, VDI/VDE - 2606 Measurement of Gearing tools - Measuring of Hobs Part 1

[13] DIN 3968, 1960, Tolerances for Single-Start Hobs for Involute Spur Gears

[14] Radzevich S. P., 2012, *Dudley's Handbook of Practical Gear Design and Manufacture*, CRC Press, Taylor & Francis Group, Boca Raton, Florida, USA.

[15] Andersson S. A. E., 1973, On the Design of Internal Involute Spur Gears, PhD thesis, Lund University, Lund, Sweden.

[16] Olsson A., 1995, On the Design of Internal Involute Helical Gears, PhD thesis, Lund Univeristy, Lund, Sweden.

[17] Fetvaci C., 2010, Definition of Involute Spur Gear Profiles Generated by Gear-Type Shaper Cutters, Mechanics Based Design of Structures and Machines, 38, pp. 481–492.

[18] Tsay C. B., Liu W. Y. and Chen Y. C., 2000, Spur Gear Generation by Shaper Cutters, Journal of Materials Processing Technology, 104, pp. 271–279.

[19] Dudley, D. W., 1962, Gear Handbook: The Design, Manufacture, and Application of Gears, 1st ed., McGraw-Hill, New York, USA.

[20] Michalski J., Skoczylas L., 2008, Modelling the Tooth Flanks of Hobbed Gears in the CAD Environment, Int J Adv Manuf Technol, 36:746–751

[21] Bergseth, E., 2007, Virtual Hobbing, OST-07 Symposium on Machine Design, Tallin

[22] Gravel G., 2013, Simulation of Deviations in Hobbing and Generation Grinding, International Conference on Gears, VDI-Berichte 2199.1, pp. 367-378

[23] DIN 3962, 1978 Tolerances for Cylindrical Gear Teeth - Part 1.

[24] DIN 3962, 1978 Tolerances for Cylindrical Gear Teeth - Part 2.

[25] Volvo Group Standard, 2007, STD 5082,81: Deviations and Inspection Methods for Cylindrical Gears with Involute Gear Teeth, pp 1-23.

[26] Lange, J., 2009, How Are You Dealing with Bias Error in Your Helical Gears?, Gear Technology, Vol. 26, No. 3, pp. 47–54.

[27] Klocke F., Brumm M., Hellman M., 2014, Improvement of the design method for Helical Gears by Considering Manufacturing Related Bias Errors, International Gear Conference, 2014, Lyon, France.

[28] Ståhl, J-E, (2012), *Metal Cutting – Theories and Models* Division of Production and Materials Engineering, Lund University in Cooperation with Seco Tools AB, Textbook, Lund/Fagersta, Sweden.

[29] Hoffmeister B., 1970, Über den Verschleiss am Wälzfräser, Ph.D. thesis, der Rheinisch-Westfalischen Technischen Hochschule Aachen, Germany

[30] Fette, 2015, Fette - Gear Cutting Tools, Leitz Metalworking Technology Group, Fette GmBH, Schwarzenbek, Germany

[31] Sulzer, G., 1973, Leistungssteigerung bei der Zylinderradherstellung durch genaue Erfassung der Zerspankinematik, Ph.D. thesis, Technischen Hochschule, Aachen, Germany.

[32] Antoniadis A., Vidakis N., and Bilalis N., 2002 Fatigue Fracture Investigation of Cemented Carbide Tools in Gear Hobbing, Part 1: FEM Modeling of Fly Hobbing and Computational Interpretation of Experimental Results, ASME Journal of Manufacturing Science and Engineering, 124:784-791.

[33] Tapoglou N., Antoniadis A., 2011, Hob3D: A Novel Gear Hobbing Simulation Software Proceedings of the World Congress on Engineering, 1.

[34] Klocke F., Weber G. T., Stuckenberg A., Krömer M., Kobialka C., 2013, Simulation-based Process Design for Gear Hobbing, International Conference on Gears, VDI-Berichte 2199.1, pp. 341-352.

[35] Sabkhi N., Pelaingre C., Barlier C., Moufki A., and Nouari M., 2015, Characterization of the Cutting Forces Generated During the Gear Hobbing Process: Spur Gear, 15th CIRP Conference on Modelling of Machining Operations, 31:411-416.

[36] Hill R., 1950, *The Mathematical Theory of Plasticity.* Oxford University Press, London, U.K.

[37] T. Özel, T. Altan, Process Simulation using Finite Element Method - Prediction of Cutting Forces, Tool Stresses and Temperatures in High - Speed Flat End Milling, International Journal of Machine Tools & Manufacture, 40:713-738, 2000.

[38] A. Svaboda, D. Wedberg, L-E. Lindgren, Simulation of Metal Cutting Using a Physically Based Plasticity Model, Modelling and simulation in materials science and engineering, 18:1-19, 2010.

[39] Dewhurst P., 1978, On the Non-Uniqueness of the Machining Process, Proceedings of the Royal Society of London, Series A, Mathematical and Physical Sciences, 360:587–610.

[40] Fang N., Jawahir I.S., and Oxley P.L.B., 2001, A Universal Slip-Line Model with Non-Unique Solutions For Machining with Curled Chip Formation and a Restricted Contact Tool, International Journal of Mechanical Sciences, 43:557–580.

[41] Altintas Y., 2012, *Manufacturing Automation: Metal Cutting Mechanics, Machine Tool Vibration, and CNC Design*, Cambridge University Press, New York, USA.

[42] Childs T., Maekawa K., Obikawa T., and Yamane Y., 2000 *Metal Machining - Theory and Applications.* John Wiley & Sons, New York, USA.

[43] Agmell M., Ahadi A., and Ståhl J. E., 2011, A fully coupled thermomechanical two-dimensional simulation model for orthogonal cutting: formulation and simulation, Proceedings of the Institution of Mechanical Engineers, Part B: Journal of Engineering Manufacture, 225(10), 1735-1745.

[44] Hanna N. H., Tobias S. A., 1974, A Theory of Nonlinear Regenerative Chatter, *ASME Journal of Engineering for Industry*, 96: 247- 253.

[45] Kienzle O., 1952, Die Bestimmung von Kräften und Leistungen an Spanenden Werkzeugen und Werkzeugmaschinen, VDI Zeitschrift, 94/11/12:299-305.

[46] Stephenson D. A., Agapiou J. S., 2006 *Metal Cutting Theory and Practice* CRC Press, Taylor & Francis Group, 2nd ed, Boca Raton, Florida, USA.

[47] Taylor F. W., 1906, *On the Art of Cutting Metals*, The American Society of Mechanical Engineers, New York, USA.

[48] Colding B., 1959, A wear relationship for turning, milling and grinding, KTH Royal Institute of Technology, Doctoral Thesis, Stockholm, Sweden.

[49] Colding, B., 1981, The Machining Productivity Mountain and its Wall of Optimum Productivity, 9th NAMRAC, 37-42.

[50] Colding B., 1991, A Tool - Temperature / Tool - Life Relationship Covering a Wide Range of Cutting Data, CIRP Annals - Manufacturing Technology, 40, 35–40.

[51] Dawson T. G., Kurfess T. R., 2006, Modeling the Progression of Flank Wear on Uncoated and Ceramic-Coated Polycrystalline Cubic Boron Nitride Tools in Hard Turning, ASME Journal of Manufacturing Science and Engineering, 128:104-109.

[52] Kishawy H. A., Kannan S., and Balazinski M., 2005, Analytical Modeling of Tool Wear Progression During Turning Particulate Reinforced Metal Matrix Composites CIRP Annals - Manufacturing Technology, 54:55-58.

[53] Usui E., Shirakashi T., and Kitagawa T., 1984, Analytical Prediction of Cutting Tool Wear, Wear, 100:129-151.

[54] Archard J. F., 1953, Contact and Rubbing of Flat Surfaces J. Appl. Phys, 24:981-988.